Annual Technical Report *March 1972*

DYNAMIC TENSILE FAILURE IN ROCKS

Prepared for:

BUREAU OF MINES
TWIN CITIES MINING RESEARCH CENTER
TWIN CITIES, MINNESOTA 55111

Sponsored by

ADVANCED RESEARCH PROJECTS AGENCY
ARPA ORDER 1579, AMENDMENT 2
PROGRAM 1F10

STANFORD RESEARCH INSTITUTE
Menlo Park, California 94025 · U.S.A.

DOCUMENT CONTROL DATA - R & D

(Security classification of title, body of abstract and indexing annotation must be entered when the overall report is classified)

1. ORIGINATING ACTIVITY (Corporate author)
Stanford Research Institute
Menlo Park, California 94025

2a. REPORT SECURITY CLASSIFICATION
UNCLASSIFIED

2b. GROUP

3. REPORT TITLE

DYNAMIC TENSILE FAILURE IN ROCKS

4. DESCRIPTIVE NOTES (Type of report and inclusive dates)
Annual Technical Report February 12, 1971 through February 11, 1972

5. AUTHOR(S) (First name, middle initial, last name)
Donald A. Shockey, Carl F. Petersen, Donald R. Curran and John T. Rosenberg

6. REPORT DATE
March 11, 1972

7a. TOTAL NO. OF PAGES
80

7b. NO. OF REFS
41

8a. CONTRACT OR GRANT NO.
H0210018

b. PROJECT NO.
1579, Amendment 2

c.
1F10

d.

9a. ORIGINATOR'S REPORT NUMBER(S)
PYU-1087

9b. OTHER REPORT NO(S) (Any other numbers that may be assigned this report)

10. DISTRIBUTION STATEMENT
Unlimited

11. SUPPLEMENTARY NOTES

12. SPONSORING MILITARY ACTIVITY
Advanced Research Projects Agency
Washington, D.C. 20301

13. ABSTRACT

A simple homogeneous rock, Arkansas novaculite, was chosen for dynamic tensile failure studies. Experimental techniques for performing dynamic tensile tests on rocks were developed and used to provide meaningful measurements of dynamic tensile strength. A way to eliminate the occurrence of undesirable radial cracking of the specimen during testing was found; specimen recovery and fracture analysis methods were implemented.

Novaculite specimens were characterized with respect to static and dynamic fracture strength, fracture toughness, defect and microstructure, and other properties and parameters pertinent to the fracture behavior. A particularly important accomplishment was the quantitative determination of the size distribution of inherent cracklike defects, for this is thought to play a dominant role in the comminution characteristics of the rock, and is thus a necessary parameter for a dynamic fracture model. The quasi static tensile strength was determined by means of expanding ring tests to be 440 ± 20 kg/cm^2. The tensile fracture strength of novaculite was measured in high loading rate gas gun experiments to be 410 ± 20 kg/cm^2 and found to be independent of defect orientation. Thus the tensile fracture strength is strain rate insensitive in the range 10^{-4} to 10^{4} sec^{-1}. A Griffith-Irwin type relation is suggested for the failure criterion under dynamic loads $\sigma_f = 10^2 c_{max}^{-1/2}$ where σ_f is the fracture strength in kilograms/cm^2 and c_{max} is the maximum crack radius in centimeters.

(continued)

14 KEY WORDS	LINK A		LINK B		LINK C	
	ROLE	WT	ROLE	WT	ROLE	WT
Dynamic tensile test						
Tensile strength						
Novaculite						
Fracture toughness						
Gas gun						

ABSTRACT (concluded)

The fracture mechanism in novaculite under dynamic tension was deduced from fractographic observations to consist of the following sequence of events: (1) activation of preexisting cracklike defects, (2) growth of individual cracks radially outward, (3) coalescence of neighboring cracks, and (4) fragmentation of the sample. Based on this mechanism a dynamic fracture model has been partially developed. According to this model, the most influential parameters affecting the comminution characteristics of rock are the size distribution of preexisting cracks, the applied stress and stress duration, and the inherent fracture resistance of the rock. It is hoped that these quantities can be related by means of the dynamic fracture model to predict resultant fragment size distributions.

During this first year, considerable effort was placed on determination of the quantities associated with the activation and growth stages of the model. In the second year, the crack coalescence and fragmentation stages will be treated, and the dynamic fracture model will be completed. The applicability of the model to rocks in general will be tested by performing experiments on other rock types.

STANFORD RESEARCH INSTITUTE
Menlo Park, California 94025 · U.S.A.

March 11, 1972

Annual Technical Report
Covering the Period February 12, 1971 through February 11, 1972

DYNAMIC TENSILE FAILURE IN ROCKS

By: Donald A. Shockey, Carl F. Petersen, Donald R. Curran and
John T. Rosenberg

Prepared for: Bureau of Mines
Twin Cities Mining Research Center
Twin Cities, Minnesota 55111

Attn: Dr. D. E. Siskind

SRI Project PYU-1087

ARPA Order Number:	1579, Amendment 2
Program Code Number:	1F10
Name of Contractor:	Stanford Research Institute
Date of Contract:	February 12, 1971
Contract Expiration Date:	February 11, 1972
Amount of Contract:	$73,151
Contract Number:	H0210018
Principal Investigator:	Dr. Donald R. Curran
Phone Number:	(415) 326-6200, Ext. 4560
Project Scientist:	Dr. Carl F. Petersen
Phone Number:	(415) 326-6200, Ext. 4614
Short Title of Work:	Dynamic Tensile Failure in Rocks

Sponsored by Advanced Research Projects Agency

Approved:

George R. Abrahamson, Director
Poulter Laboratory

C. J. Cook, Executive Director
Physical Sciences Division

ABSTRACT

This report presents the results of the first year of a three-year experimental and theoretical program to study dynamic tensile failure of rock. Techniques for loading rock specimens in tension at high rates in a gas gun, and recovering them are described. Ytterbium stress gages were used to determine loading histories and measure dynamic tensile strengths.

All experiments were carried out on Arkansas novaculite, a quartzite chosen for its simple homogeneous structure. The fracture mechanism is inferred from the results of fractographic examinations of recovered specimens, and a computational model for dynamic tensile fracture in rock based on the hypothesized fracture mechanism is proposed and partially developed. Future work is aimed at further development and generalization of this model to allow predictions of fragment size distributions in rock from known dynamic tensile loading histories.

CONTENTS

FIGURES

FIGURES (concluded)

TABLES

INTRODUCTION

Fracture in rock under high rate tensile loading conditions is more complex and considerably less well understood than fracture under quasi-static conditions. There is at present no satisfactory theoretical basis for predicting dynamic failure behavior, although the advantages of having such a basis are many. An understanding of rock failure under dynamic tensile loads would be most useful in the solution of practical mining and civil engineering problems. With such knowledge rapid excavation could be done more safely and economically, the stability of structures in rock could be designed and evaluated with more confidence, and the efficiency of rock disintegration processes could be improved. It is thus the objective of this three year program to develop a model for rock fracture which can be used to predict failure behavior under high rate tensile loading.

This report describes the progress made during the first year. In this section we discuss the strength of rocks, compare their fracture behavior under quasi-static and high rate loads, and review previous attempts to model dynamic fracture of materials in general. Properties and microstructural features of Arkansas novaculite, the specimen material, are given in Section II, the results of high rate loading experiments are presented in Section III, a fracture mechanism is proposed in Section IV, and a dynamic fracture model is outlined in Section V. Plans for improving and substantiating this model are stated in Section VI.

The Quasi-Static Strength of Rocks

Generally speaking, there is no well-defined yield strength or fracture strength for rock materials. Strength values measured on ten or twenty similar rock samples may vary by more than an order of magnitude, even when extreme care is taken to ensure that the samples are as much alike as possible.[1] Therefore, rocks cannot in general be characterized

by a single strength value as is usually possible with metals, and it is of little help to use a criterion such as "Fracture occurs when the fracture strength of the material is exceeded."

The main reason for the large scatter in the measured strengths of rocks is most probably the wide range in the sizes of inherent, internal cracks. It is well established that preexisting cracks control the strength of brittle or semibrittle materials and that the larger the cracks, the weaker the material. In particular, the size of the largest crack determines the quasi-static fracture strength. Rocks typically have a very pronounced defect structure, whose size range is much broader than that typical of metals.

Deliberate processing procedures for metals control the maximum flaw size; hence the fracture strength of metal is rather constant from quantity to quantity. In contrast, the haphazard conditions under which naturally occurring rock is formed result in a wide distribution of flaw sizes and corresponding scatter in fracture strengths. Thus in formulating a predictive capability for tensile failure in rocks, it is necessary to take into account the size distribution of inherent cracks.

The Griffith theory[2] links the sample strength with the size of the maximum crack and provides the most reliable expression for predicting quasi-static fracture in rock. The two main assumptions of the theory, (1) that the material is linear and elastic and (2) that the material contains a population of flaws, are well satisfied in most rocks. Griffith related the brittle fracture stress σ to the elastic modulus E, the surface energy γ, and the radius of the largest crack c, in the following way:

$$\sigma = k \sqrt{\frac{E\gamma}{c}}$$

where k is a geometrical constant* of the order of one.

* k does in fact contain the Poisson ratio, but since variations in this property from rock to rock are usually insignificant, k may be considered to depend only on specimen geometry.

Since all material properties are contained in the product $(E\gamma)^{\frac{1}{2}}$, this term characterizes the response of the material to fracture. Specifically, $(E\gamma)^{\frac{1}{2}}$ is the material property that indicates the basic propensity of the material for brittle tensile failure. In fracture mechanics terminology[3,4] it corresponds to the critical stress intensity factor K_{Ic}.

$$\sigma \propto K_{Ic}/c^{\frac{1}{2}}$$

This inherent fracture resistance may be considered a material property, but it is not necessarily a material constant. In general, its value is a function of geometry, strain rate and temperature.

According to the Griffith theory or the concepts of fracture mechanics, the quasi-static strength of a rock sample can be predicted knowing (1) the inherent fracture resistance of the rock $(E\gamma)^{\frac{1}{2}}$ or K_{Ic} and (2) the size of the largest most favorably oriented flaw in the sample. The inherent fracture resistance may be evaluated either by measuring the elastic modulus and the fracture surface energy individually in separate experiments, or by measuring the strength of a specimen in which the maximum flaw size is known. Statistical methods are usually employed to determine the maximum flaw size. A Scheil-type[5,6] statistical transformation of flaw traces on sectioned surfaces will be shown to have particular application to the present work.

Failure of Rocks Under Dynamic Tensile Loads

High rate loading occurs, for example, when explosive in contact with a sample is detonated or when a sample is subjected to high velocity impact. Under these conditions fracture is induced by tensile stresses arising from intersections of reflected shock waves. Such tensile stresses typically have rise times of the order of tens of nanoseconds and endure for several tenths of a microsecond, during which time activated cracks grow. The extent to which individual cracks propagate and coalesce depends predominantly on the duration of the stress pulse; thus time as well as stress plays an important role in the dynamic fracture criterion.

Dynamic tensile failure in metals, where large numbers of microcracks form but do not fragment the specimen, has received considerable attention, and several schemes have been proposed to include time in dynamic fracture criteria.[7-13] A general method was presented by Tuler and Butcher[14] and by Gilman and Tuler,[15] proposing that a damage function Φ is a function of the entire stress history

$$\Phi = \int_{-\infty}^{t} f(\sigma(t))\, dt \qquad (1)$$

where Φ is selected to be any convenient function of damage. For example, Φ could be the total number or volume of the microcracks formed. It was suggested that $f(\sigma(t))$ be expanded in powers of $\sigma-\sigma_o$, where σ_o is a threshold stress below which no damage will occur regardless of stress duration. It was further suggested as a zero order approximation that one term might be expected to be dominant, so that

$$\Phi = \int_{-\infty}^{t} (\sigma-\sigma_o)^{\lambda} dt \qquad (2)$$

where λ and σ_o are considered material constants determined by experiment. Much effort has been expended in trying to relate observed shock-induced damage thresholds in metals to Eq. (2). Usually Φ is picked to be a level of microscopic damage visible at some level of magnification, and λ is chosen to be a number that fits the data.[10,16-18] The results have been only partially successful, which is perhaps to be expected since the definition of Φ is very qualitative and a given material is described by only two parameters. In short, Eq. (1) is undoubtedly general enough to be correct in principle, but Eq. (2) does not contain enough information about a given material to be useful other than as a method for describing experimental results.

Recently an approach was introduced at SRI[19-21] that is consistent with the basic approach of Tuler and Butcher, but concentrates on more precise physical definitions of the Φ and f functions in Eq. (1) than has been used before. This approach has yielded promising results for both ductile and brittle metals. In addition, the simple physical model underlying the approach allows dynamic fracture phenomena to be related to quasi-static fracture behavior, and thus suggests the possibility of eventually understanding the nucleation and growth of microcracks resulting in fracture at all rates of loading. The details of the SRI dynamic fracture model and its application to rocks are discussed below.

The SRI Dynamic Fracture Model

Postfracture examination of metallic and polymeric specimens subjected to flat plate impact revealed that under dynamic loading conditions fracture originates at many sites throughout the specimen.[19-22] Each small crack then propagates and achieves a certain size before the stress pulse vanishes. We noted the analogy to a metallurgical phase transformation, in which second-phase particles nucleate and grow within a matrix material under the influence of a thermodynamic driving force, and developed a model based on this analogy. Thus the development of fracture damage was treated as a process of crack nucleation and growth. We have not yet treated in detail the third stage in the fracture mechanism, coalescence, in which individual cracks meet and join up. This stage is particularly important for more brittle materials in which fragmentation occurs.

Stress dependent crack nucleation and growth rate functions have been experimentally determined for several metals[19-21] and for one polymer.[22] These functions govern the development of fracture damage and can be used to predict the extent and location of damage that will result from an arbitrary loading history.

The nucleation rate and growth rate functions were determined from experiments using known stress histories. The stress history was calculated using a PUFF code[23] with appropriate constitutive relations. Unmodified constitutive relations for the material can be used to calculate the stress history for small amounts of damage. However, for even moderate damage levels the effect of the damage on the stress history is significant, and a modified equation of state should be used that treats the material as a porous solid consisting of damaged regions and undamaged regions.

After loading by a known pulse, the specimen is sectioned on a plane parallel to the impact direction to reveal the damage in cross section. Ductile fracture damage appears as spherical voids, and brittle fracture damage appears as plane cracks. An important aspect of the analysis is determination of the volume distribution of damage from such surface observations. The procedure for developing a predictive capability for fracture by stress waves was:

- load dynamically and recover specimens
- achieve experimental control so that the damage can be stopped in different stages of growth
- describe quantitatively the size and the spatial distribution of damage in the volume of the material
- specify the macroscopic stress and the stress duration at any location in the specimen under conditions of nucleation and growth of damage.

Nucleation rate and growth rate functions have been determined completely by combining the information gained in the steps above. Moreover, theoretical work in the nucleation and growth processes has made it possible to obtain estimates of these functions for materials other than those tested.

For material that fractures in a ductile manner under dynamic loading, the experimental data suggested that the void nucleation rate $\dot{N}$ has the following form[20]

$$\dot{N} = \dot{N}_o \exp \frac{\sigma - \sigma_{No}}{\sigma_1}$$

where σ is the applied dynamic stress, σ_{No} is the threshold stress for void nucleation, and $\dot{N}_o$ and σ_1 are constants. This form of nucleation function is consistent with static results in which no voids appear for stresses less than the yield or ultimate strength. It not only effectively described the nucleation of voids in ductile materials, but also was successful in describing crack nucleation in more brittle materials.[20]

The growth rate of brittle cracks might be expected to differ considerably from that of a void in a ductile material. For ductile metals, voids were found experimentally to expand according to a viscous growth law

$$\dot{c} = \frac{\sigma - \sigma_{Go}}{4\eta} c$$

where σ_{Go} is the threshold stress for void growth and η is the material viscosity. Surprisingly, materials that failed by propagation of brittle-type cracks were also well described by this relation and were poorly described by brittle growth laws based on assumptions of elasticity.

Application of the SRI Dynamic Fracture Approach to Rocks

In any attempt to model dynamic fracture of rock materials, several new features must be taken into account. First, a much more pronounced inherent defect structure exists in rocks than in fabricated materials such as metals and polymers. The defect structure profoundly influences the strength and fragmentation characteristics of the rock and therefore

must be determined. Second, rocks generally fracture in a more brittle manner with more rapid crack velocities. Thus it may be difficult to stop individual cracks from growing together and extending to specimen boundaries, making it difficult to recover intact specimens for damage evaluations. Finally, increased propensity of cracks in rock to run together requires not only that crack nucleation and growth functions be obtained, but also that the third stage of the fracture process, crack coalescence, be treated. A correct model of the coalescence behavior would permit calculation of the fragment size distributions resulting from known dynamic tensile loads.

We have begun in the present work to apply the concepts of crack nucleation and growth to treat dynamic tensile failure of rock. The steps taken during the first year of the three-year program to develop a computational model for high rate fracture in rock were as follows:

- A specimen material was chosen and quantitatively characterized with respect to structure and properties.
- High rate tensile tests were performed to measure dynamic stress histories and to observe the fracture behavior.
- Fractographic analyses were carried out on tested specimens to determine the fracture mechanism.
- Construction of a computational model was begun for predicting the failure behavior under high rate tensile loads.

II CHARACTERIZATION OF ARKANSAS NOVACULITE

Microstructure

Arkansas novaculite--a naturally occurring, polycrystalline quartz--is a mineralogically simple rock, consisting of a chemically simple mineral, and was therefore a suitable material with which to begin these studies. Metallographic examination of polished and etched surfaces at 1000X shows that novaculite consists of equisized, equiaxed, and randomly oriented quartz grains having an average diameter of about 10 μ.

Figure 1 shows a polished surface that was etched for 2 minutes in 40% HF at room temperature to reveal the grain structure. Black areas are holes where natural flaws intersect the surface or where grains have been pulled out during the polishing process. Bright areas are caused by reflected light from internal surfaces. Observation of fracture surfaces with the scanning electron microscope reveals the grain structure even more clearly (Section IV). Crack propagation occurs intergranularly, exposing individual grains in the fracture surfaces.

Defect Structure

From casual observation of polished surfaces with the unaided eye, it is apparent that natural novaculite has a defect structure and that the defects are strongly oriented. Figure 2, a composite photograph at low magnification, illustrates this. Closer examination with a microscope shows that defects are present on essentially two distinguishable size levels: the larger defects have dimensions of a few hundred microns; smaller defects are roughly the size of the grains.

By exploiting the translucency of novaculite and focusing into the material to a depth of about 100 μ, we found that the larger flaws exist in two dominant shapes: plates and rods. Best results were obtained by viewing the specimen in reflected polarized light through a microscope slide and a film of matching refractive index oil (n = 1.55) on the specimen surface. Figure 3 shows a rodlike and a platelike flaw slightly

FIGURE 1 MICROSTRUCTURE OF ARKANSAS NOVACULITE SHOWING THE EQUIAXED QUARTZ GRAINS

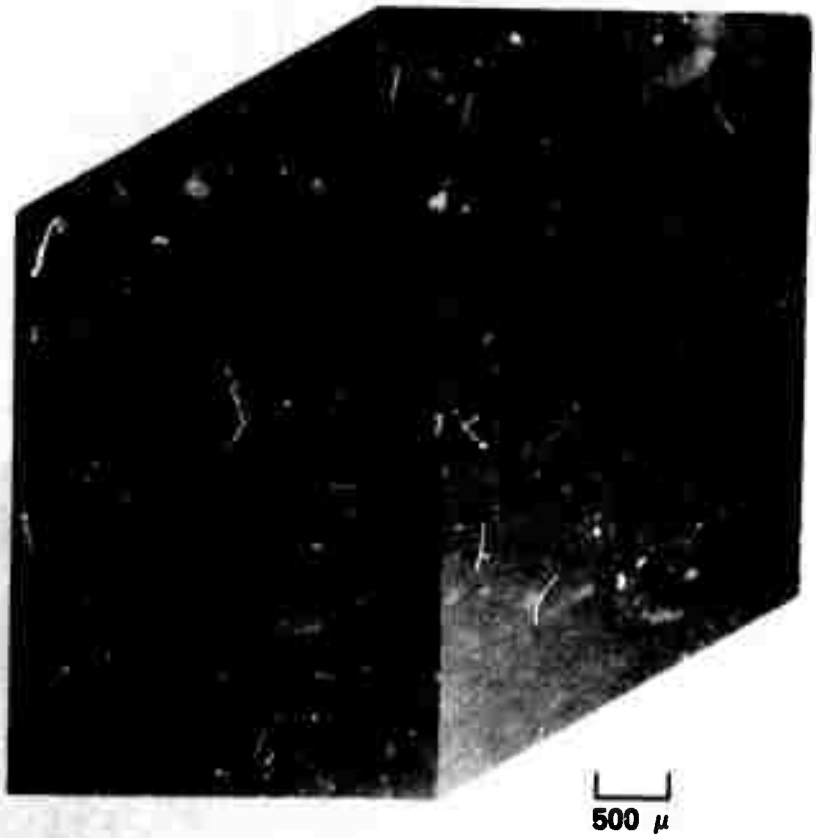

FIGURE 2 COMPOSITE MICROGRAPH OF A BLOCK OF NOVACULITE SHOWING THE PREFERRED ORIENTATION OF THE INHERENT DEFECTS

(a)

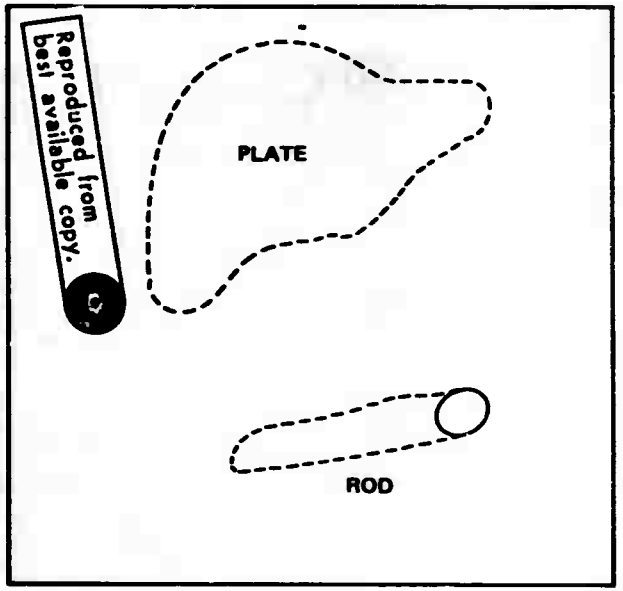

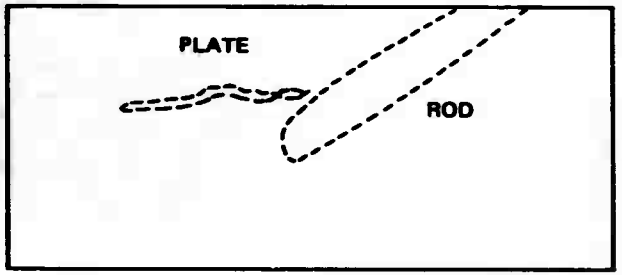

(b)

MP-1087-9

FIGURE 3 PLATELIKE AND RODLIKE INHERENT DEFECTS NEAR THE SURFACE OF NOVACULITE

below the surface of polish and inclined at an angle to it, so that only a section of each is in focus. The planes of the rather homogeneously distributed platelike flaws are roughly parallel to one another, and most of the rodlike defects are inclined at about 45° to these planes. (Rodlike flaws possibly originate from tiny bubbles of water that are rejected during crystallization of the rock and coalesce to form capillary tubes.)[24] The size distribution of these flaws was determined and is discussed later. The plates would appear to be particularly effective crack starters, and their strong preferred orientation is expected to result in highly anisotropic fracture properties.

Determination of Maximum Crack Size

As has been mentioned, the size of the largest flaw existing in a specimen determines to a large extent its quasi-static strength. Thus in establishing a failure criterion it is necessary to be able to establish the maximum crack size. For opaque materials this is a formidable task. A number of techniques have potential for providing pictures of internal artifacts in opaque materials. These include methods based on holography, ultrasonic imaging, infrared photography and x-ray topography. However, these imaging methods are still in the early stages of development, and it is difficult to have much confidence in the accuracy of the results.

A better established approach is to section the rock specimen perhaps on three perpendicular surfaces and measure the crack traces intersecting a sufficiently large area of the surfaces of section. If many crack traces are observed whose average length is not greatly exceeded by any one trace, then statistically, the maximum crack diameter is approximately equal to the length of the largest trace.

Such conditions seem to prevail in Arkansas novaculite; seldom was any crack trace observed whose length exceeded greatly those of many other crack traces. The largest penny-shaped crack in the sample of novaculite used in this work was established in this way to be about 500 μ in diameter.

Determination of the Initial Crack Size Distribution

Under high rate loading conditions, cracks smaller than the largest crack may be activated and contribute to specimen failure. Thus in developing a capability to predict fracture behavior of rock under dynamic loads, it is necessary to be able to determine the size distribution of inherent flaws. As was done in the determination of the maximum crack size, novel imaging techniques were rejected in favor of the cheaper and more reliable technique of statistically transforming artifacts on surfaces of section.

The traces of cracks as seen in a composite photograph of a sectioned and polished rock surface were counted and measured. These data were then statistically transformed to obtain the size distribution of inherent cracks per unit volume.

Nine overlapping photographs at 40X were required to span the diameter of a rock specimen. The total photographed area was slightly more than 1.1 cm^2, and in this area 194 preexisting crack traces were counted and measured. These data were converted by means of a Scheil type statistical transformation[3,4] implemented by the BABS2 computer code developed at SRI; the results are presented in Figure 4.

Here the cumulative concentration of cracks having radii greater than radius c_i is plotted as a function of c_i. The relatively few (194) traces observed on about 1 cm^2 of the surface of section transform into a very large volume density (~100,000/cm^3). The size distribution of preexisting cracks has a parabolic form in log-normal space with a cutoff at about $c = 500\ \mu$. The curve is well described by the analytical expression

$$N = \delta(c)\ \exp[11.1 - (3.7 \times 10^{2})c + (0.42 \times 10^{4})c^{2}] \qquad (3)$$

where $\delta(c) = 1$ for $0 < c \leq 0.05$

$\delta(c) = 0$ for $c > 0.05$

and c is in centimeters.

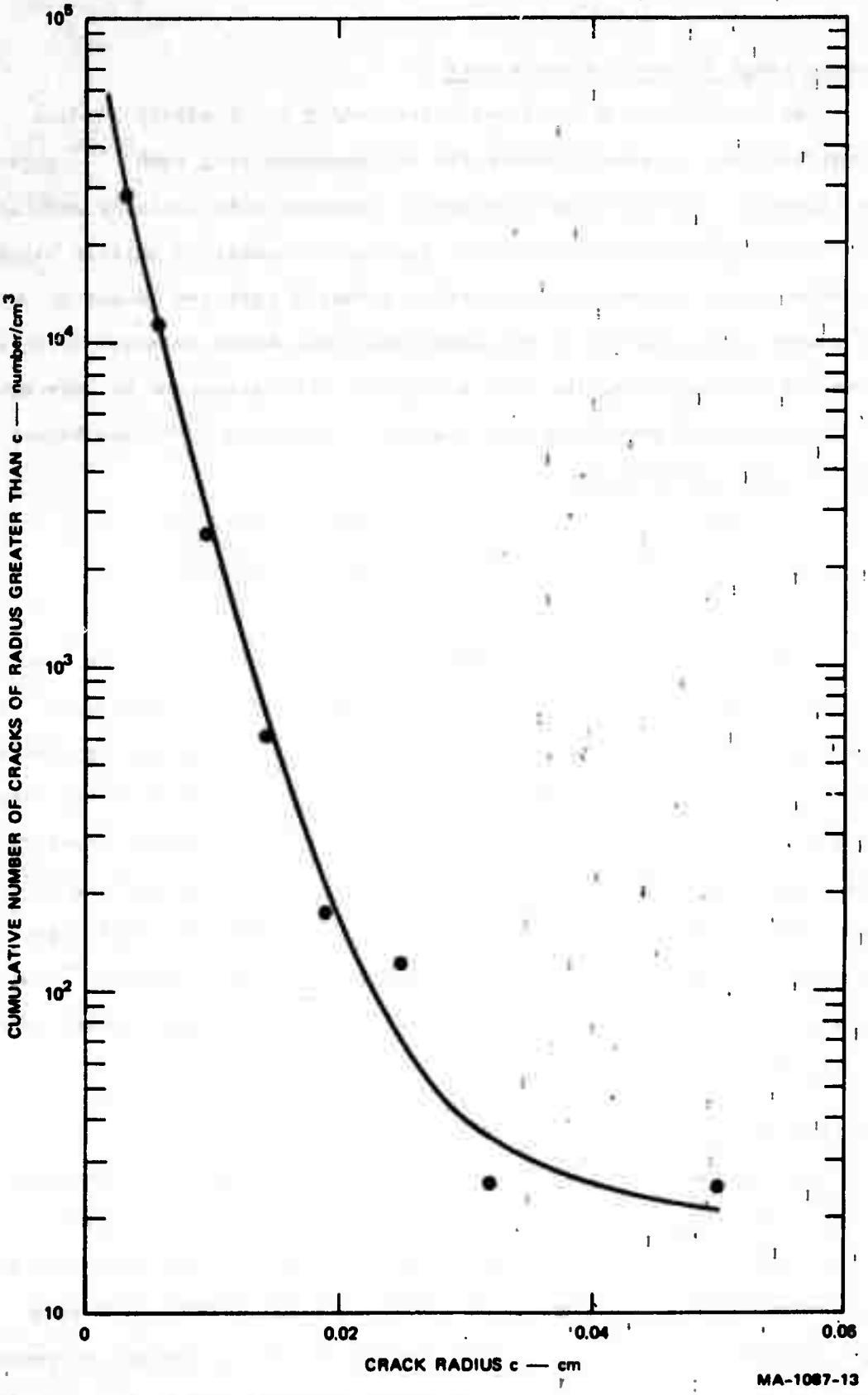

FIGURE 4 SIZE DISTRIBUTION OF INHERENT FLAWS IN ARKANSAS NOVACULITE

Quasi-Static Strength Measurements

The tensile strength of novaculite under quasi-static loading conditions was determined using the SRI expanded ring test[25,26] shown in Figure 5. In this test hydrostatic pressure acts radially against the internal wall of a cylindrical specimen to create a uniform tangential tensile stress in the specimen wall. Nonaxial stresses caused by misalignment and localized stress concentrations, which normally arise from gripping or supporting the test specimens, are eliminated in this method.

Ring-shaped specimens were diamond ground from oversized blanks to the following dimensions:

I.D.	2.000 ± 0.0005 in.
O.D.	2.300 ± 0.0005 in.
Height	0.300 ± 0.0005 in.

All strength measurements were made at a strain rate of 3×10^{-4} sec^{-1}.

Measurements were taken both in air and under a vacuum of 10^{-5} torr. Some materials show higher strengths under vacuum,[27] indicating that stress corrosion is an important factor. No significant difference was seen for novaculite. Results of 15 tests in air indicated a tensile strength of 441 ± 20 kg/cm^2 and 12 tests under vacuum indicated 448 ± 33 kg/cm^2. The extremes measured were 517 and 372 kg/cm^2. These strengths are considerably higher than those reported by Hardy and Jayaraman[28] for a variety of rocks, such as Barre granite, 88 kg/cm^2; Crab Orchard sandstone, 71 kg/cm^2; and Leuders limestone, 47 kg/cm^2.

Inherent Fracture Resistance

The longitudinal sound speed c_ℓ in novaculite was determined by the time-in-flight ultrasonic method to be 5.9×10^5 cm/sec; a value of 2.63 g/cm^3 was determined for its density. These values were used to calculate a Young's modulus E of about 6.4×10^5 kg/cm^2. Friedman and coworkers,[29] using the double cantilever beam technique, determined the fracture surface energy in Chilhowee quartzite to be about $5 \pm 2 \times 10^4$ $ergs/cm^2$.

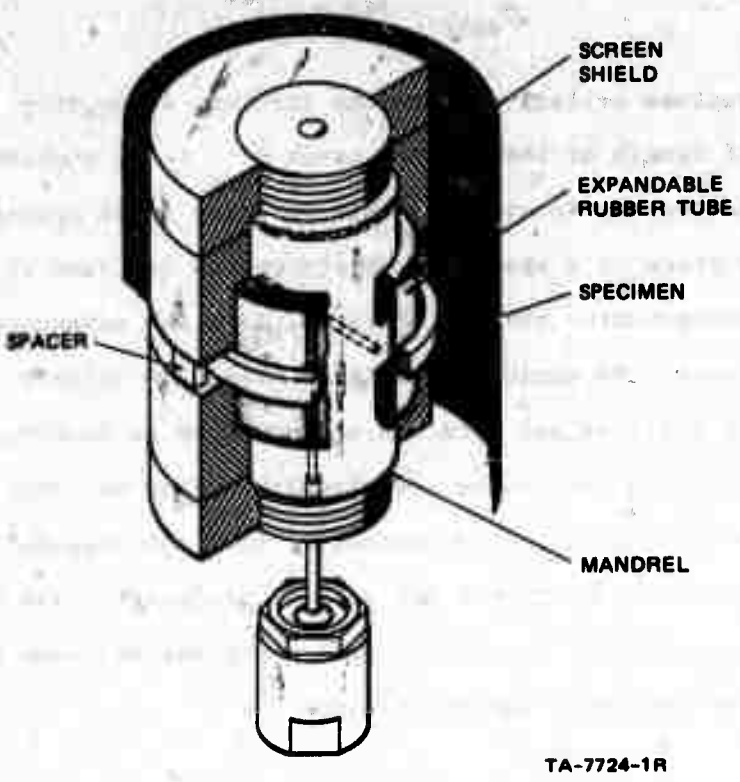

FIGURE 5 THE SRI EXPANDED RING TEST

The intrinsic fracture resistance of the rock $(\gamma E)^{\frac{1}{2}}$, which relates the fracture strength to the maximum crack size, is then about 2×10^{8} dynes $cm^{-3/2}$ or about 200 kg $cm^{-3/2}$. Substituting this value into the Griffith equation

$$\sigma_{crit} = [2\gamma E/\pi(1-\nu^2)c_{max}]^{\frac{1}{2}} \qquad (4)$$

where ν is Poisson's ratio

we establish

$$\sigma_{crit} = 160\ c_{max}^{-1/2}$$

as a fracture criterion where the fracture strength σ_{crit} is in kg/cm^2 and the half length of the largest crack c_{max} is in centimeters.

Another way to evaluate this property is to measure the size of the largest crack in a specimen, determine the fracture strength, and use fracture mechanics theory. This was done for novaculite for the quasi-static case. We could not establish fracture origins on novaculite fracture surfaces and were therefore unable to determine if edge flaws or internal flaws controlled the strength. Thus we could only estimate the fracture toughness K_{Ic} of novaculite from the measured fracture strength σ_f and the half length of the largest plate-like flaw c_{max}, by using Sneddon's relation for an internal penny-shaped crack in an infinite medium subjected to uniform tension[30]

$$K_{Ic} = \frac{2}{\sqrt{\pi}} \sigma_f \sqrt{c_{max}} \cong 110\ kg/cm^{3/2} \qquad (5)$$

as a lower bound and the expression for an edge crack in a semiinfinite sheet subjected to tension[31]

$$K_{Ic} = 1.12\ \sigma_f \sqrt{\pi c_{max}} \cong 175\ kg/cm^{3/2} \qquad (6)$$

as an upper bound.

These values are considerably lower than the value Bieniawski[32] obtained from 4-point bend tests on quartzite, 630 $kg/cm^{3/2}$, or that calculated from Friedman et al[29] measurements of the fracture surface energy, 280 ± 110 $kg/cm^{3/2}$. In view of the results of the dynamic tensile strength measurements reported in the next section, we feel that Eq. (3) is more appropriate than Eq. (4) for these tests and hence that the value of 110 $kg/cm^{3/2}$ is the more accurate. Thus solving Eq. (3) for the fracture

stress σ_f we obtain

$$\sigma_f = (98 \text{ kg/cm}^{3/2}) \, c_{max}^{-1/2}$$

for the quasi-static fracture criterion for novaculite.

The results of the characterization work for Arkansas novaculite are summarized in Table I. It remains now to determine the rate sensitivity. For rocks having low rate sensitivity, quasi-static fracture theory may describe dynamic behavior sufficiently well. Rate sensitive rocks will require a modified relation. A relation based on fracture mechanics concepts and modified to include strain rate effects has been proposed by Birkimer.[33]

Table I

STRUCTURE AND PROPERTIES OF ARKANSAS NOVACULITE

Microstructure	
Material	High purity polycrystalline quartz
Grains	Equisized, equiaxed, about 10 μ in diameter
Defect structure	
Flaw shape	Channels and plates; grain boundary seams
Size range	From ~10 to ~500 μ
Size distribution	Exponential (see Figure 4)
Maximum plate size	~ 500 μ
Preferred orientation	Very high; plates oriented on parallel planes
Physical properties	
Longitudinal sound speed	5.9×10^5 cm/sec
Density	2.63 g/cm^3
Elastic modulus	6.4×10^5 kg/cm^2
Mechanical properties	
Quasi-static fracture strength	440 ± 20 kg/cm^2
Surface energy[a]	$5 \pm 2 \times 10^4$ ergs/cm^2
Inherent fracture resistance	~110 kg/cm$^{3/2}$

[a] Reference 29.

III DYNAMIC EXPERIMENTS

High Rate Loading

High rate loading of rock specimens was accomplished in a gas gun. Projectiles, 12 inches long by $2\frac{1}{2}$ inches in diameter for the smaller gas gun and 30 inches long by 4 inches in diameter for the larger, were accelerated down the evacuated barrel of the gun by the sudden release of pressure from an adjacent pressurized chamber of helium. Flat target specimens were impacted with thin polyethylene or plexiglass flyer plates attached to the leading edge of projectiles (Figure 6). Under such flat plate impact, compressive waves initially run into the specimen and projectile head to produce a state of one-dimensional compressive strain Tension is produced in the specimens when release waves running inward from the free surface of the specimen, or from the boundary of the lower shock impedance backing material, meet similar release waves running inward from the back surface of the flyer plate (Figure 7). Knowledge of the shock impedance (product of density and shock velocity) of the rock and flyer plate (and backing material when used) allows the flyer thickness to be designed so that tension occurs first at the midplane of the specimen. A sufficiently large diameter-to-thickness ratio for the specimen ensures that the tensile strain is one-dimensional by preventing unloading waves from the specimen periphery from reaching the interior during the tension phase.

The target specimens were short cylinders, usually about 1/4-inch thick and 1/2 to 1-1/2-inches in diameter. Their axes were carefully aligned to coincide with that of the gun barrel to ensure flat plate impact. The specimens were fit tightly into constraining rings of aluminum which is a very close match to novaculite in shock impedance. Most of the aluminum constraining rings had an 8^{o} taper on the outer circumference and were press-fitted into a larger aluminum plate serving as a specimen holder. Others had no taper and were lightly held

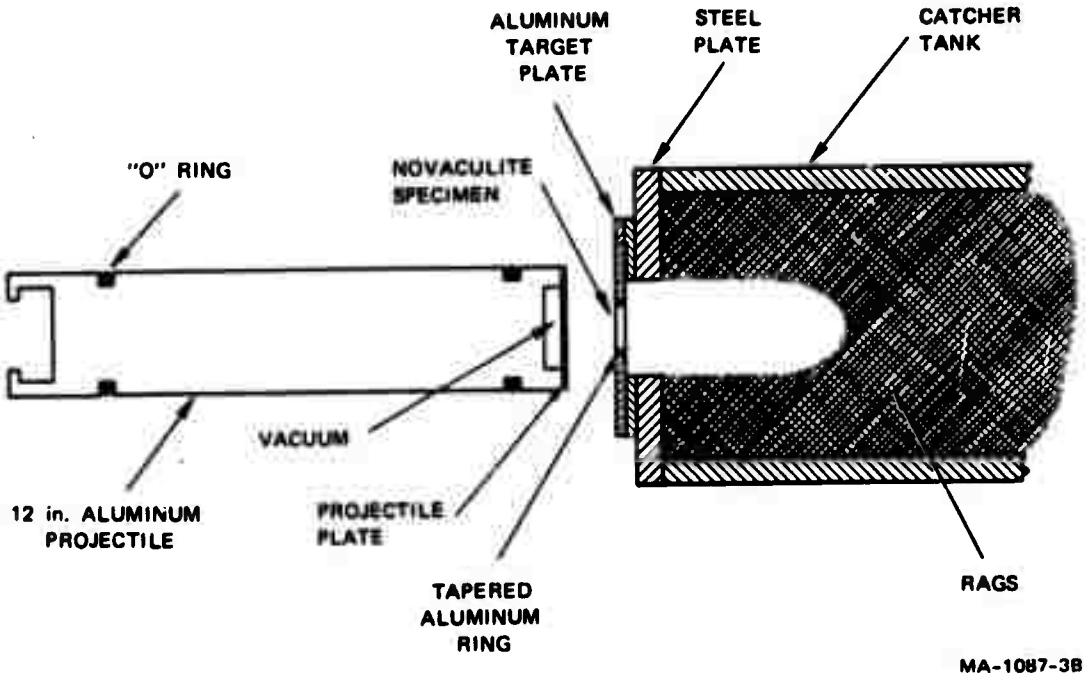

FIGURE 6 EXPERIMENTAL ARRANGEMENT FOR HIGH RATE TENSILE TESTING OF CYLINDRICAL ROCK SPECIMENS IN A GAS GUN

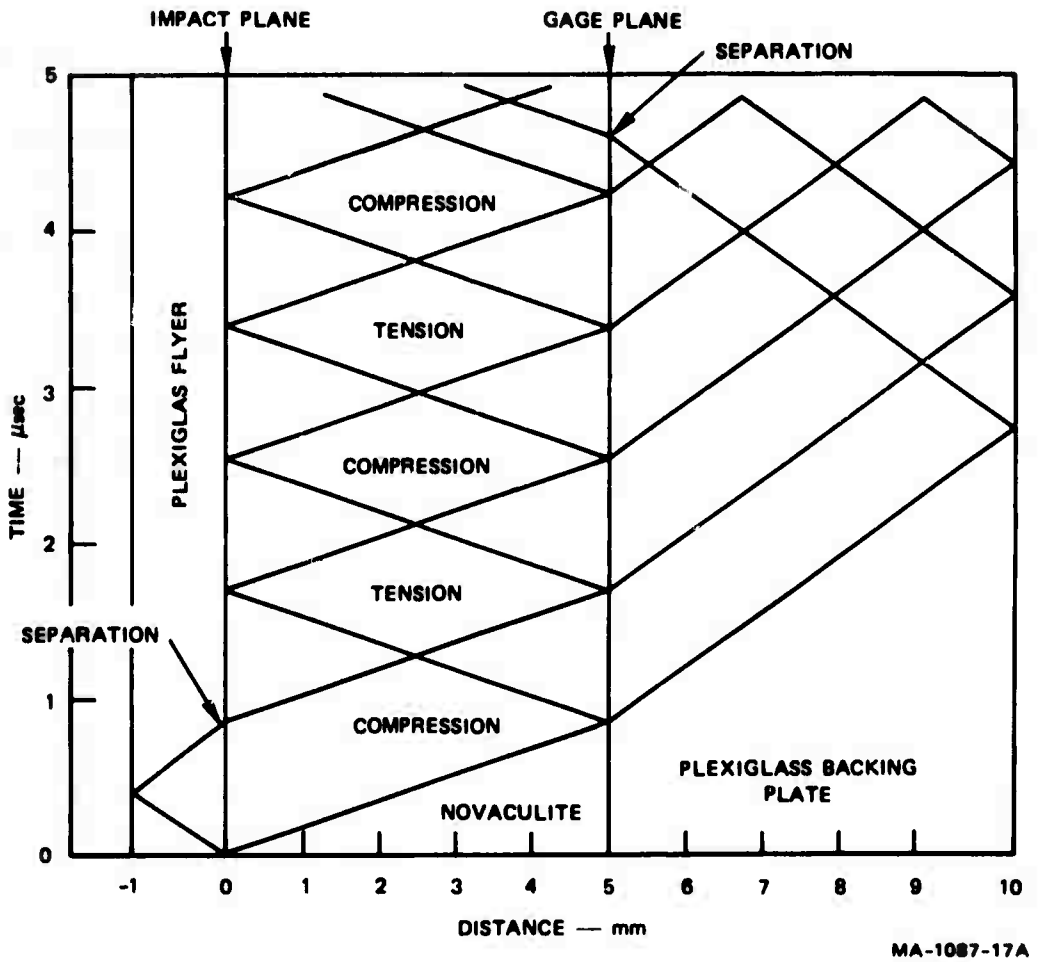

FIGURE 7 SCHEMATIC DEPICTION OF THE STRESS HISTORY OF A SPECIMEN, FLYER PLATE, AND BACKING MATERIAL CAUSED BY IMPACT

in the specimen holder by several dabs of epoxy. Upon impact with the flyer plate, the specimen and constraining ring fly free from the aluminum holder and into a catcher tank, which is lined with rags to prevent subsequent impacts and possible uncontrolled damage. The projectile and projectile head are prevented from entering the catcher tank by the steel plate.

Stress History Measurement

Piezoresistant ytterbium gages, recently developed at SRI[34,35] to measure compressive stress in the sub- and low-kilobar range, were used to measure the stress histories (peak stress and stress duration) produced in the specimens by the impact. A small grid-like gage having a resistance of 1 ohm, a thickness of 0.002 inch, and covering a 0.2- by 0.2-inch area (Figure 8) was cemented to the back surfaces of rock specimens and backed by a plexiglass plate. Because of the location of the stress gages, the stresses measured are those in the plexiglass and are compressive. The tensile stress in the rock was then calculated from the relative shock impedances of specimen and backing material. An indirect method of tensile stress measurement is necessary since inmaterial gages that measure tensile stress directly do not exist.

The gage record for a specimen in which spall fracture has occurred yields valuable information in addition to the peak stress and stress duration. Recompression waves, emitted as spall cracks form, impinge on and reload the gage to an extent proportional to the dynamic tensile strength of the rock. Furthermore, the slope of the reloading pulse is an indication of the rate of fracture--a sharp rise corresponding to brittle behavior. Finally, the measured stress history provides important information about the constitutive relations for the rock and their rate dependence.

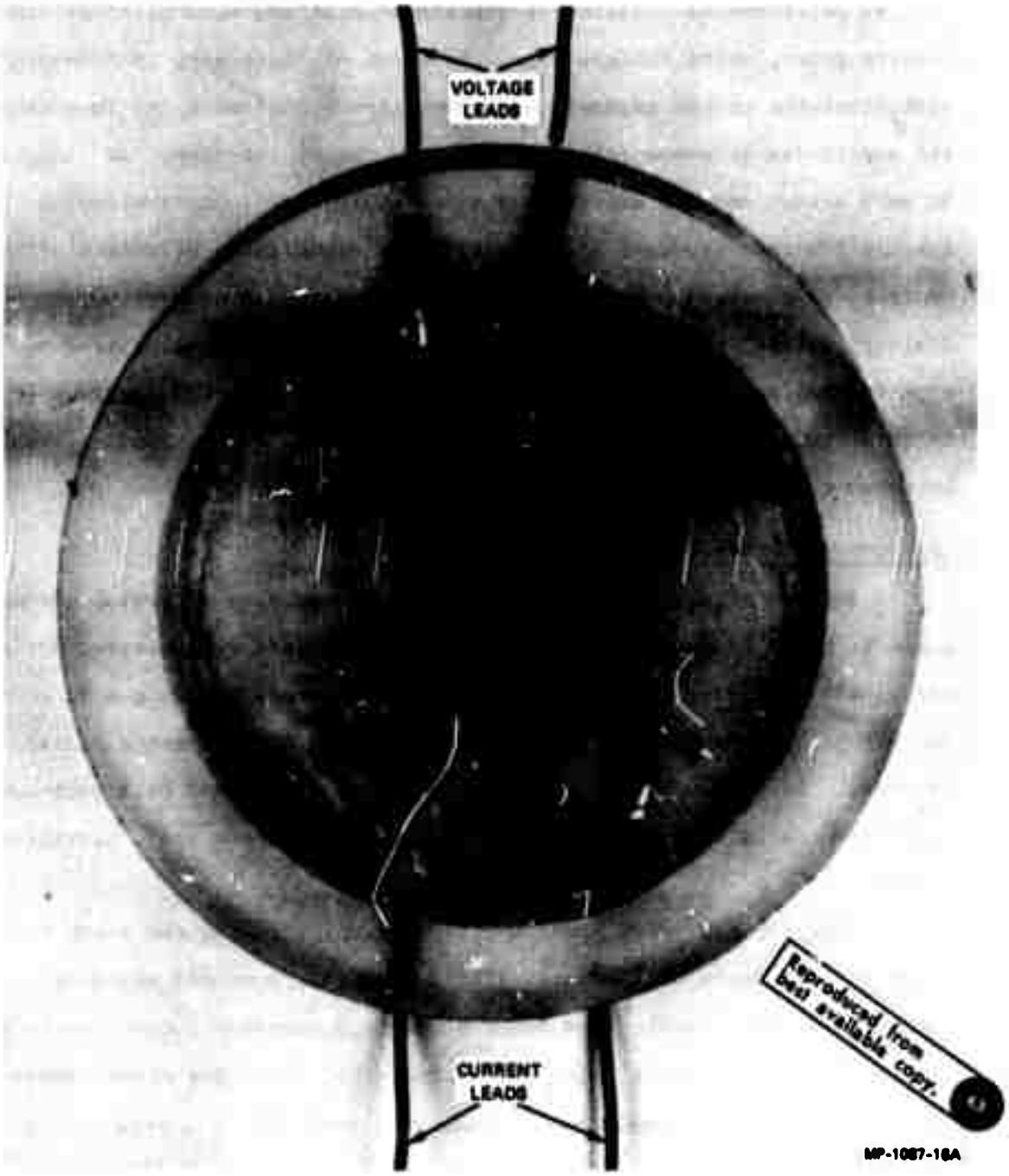

FIGURE 8 YTTERBIUM STRESS GAGE MOUNTED IN PLEXIGLASS BACKING PLATE

Dynamic Tensile Strength Measurements

We performed 43 tensile experiments on Arkansas novaculite at high loading rates, using the gas guns. Fourteen of these were instrumented with ytterbium stress gages to determine stress histories and to measure the magnitudes of recompression waves produced by fracture. An additional 20 were uninstrumented experiments whose goals were to determine the dynamic fracture strength of novaculite and any effects of defect orientation on fracture strength. The remaining nine experiments were either of a preliminary nature, to determine in a rough way the impact velocities and other experimental conditions required to carry out the proposed program, or of an investigative nature to determine, for example, the reason for the occurrence of undesirable radial cracking.

Instrumented Experiments

A summary of the 14 experiments instrumented with ytterbium stress gages is given in Table II. The first 5 experiments were carried out with the 2½-inch gas gun; the rest were done with the 4-inch gas gun to accomodate larger specimens and thicker annuli in an attempt to eliminate radial cracking. In each of these experiments the gage was used as a back-surface gage near the interface between the novaculite specimen and a plexiglass plate.

Triggering and noise problems, respectively, ruined the first two attempts at dynamic measurements (Shots 4 and 5); specimen recovery, however, was successful. The noise problems, presumably piezoelectric in origin, were overcome by using the differential recording scheme shown in Figure 9 and by separating the gage from the rock by a thin (0.010 inch) plexiglass layer. With these improvements a good record was obtained for shot 6 (Figure 10).

Table II

INSTRUMENTED DYNAMIC TENSILE EXPERIMENTS

Shot No.	Specimen Diameter (inch)	Specimen Thickness (inch)	Flyer Plate[a] (inch)	Impact Velocity (m/sec)	Calculated Peak Compressive Stress in Specimen (kg/cm^2)	Calculated Peak Tension in Specimen (kg/cm^2)	Calculated Peak Compressive Stress at Gage (kg/cm^2)	Measured Peak Compressive Stress at Gage (kg/cm^2)	Remarks
4	1.0	0.188	0.025	46.0	640	420	220	-- -	Spall
5	1.0	0.188	0.025	28.7	390	250	140	-- -	Spall
6	1.0	0.188	0.025	30.5	410	270	140	080	No spall
11	1.0	0.188	0.045	23.5	630	410	220	150	No spall
12	1.0	0.188	0.045	30.6	810	540	290	710	No spall
15	1.25	0.3	0.050	40.0	1070	700	370	530	Spall
16	1.25	0.3	0.075	24.2	650	430	220	170	Spall
17	1.25	0.3	0.075	34.9	940	620	320	560	Spall
18	1.25	0.3	0.075	32.6	870	570	300	090	Spall
19	1.0	0.3	0.075	34.0	910	590	320	-- -	Spall
20	1.0	0.3	0.075	32.2	860	560	300	240	Spall
21	1.0	0.3	0.075	35.4	950	620	330	070	Spall
22	1.25	0.3	0.075	35.7	960	630	330	420	Spall
23	1.0	0.3	0.075	29.4	790	520	270	290	Spall

a The flyer plate material was plexiglass except that for shots 4, 5, and 6 polyethylene was used.

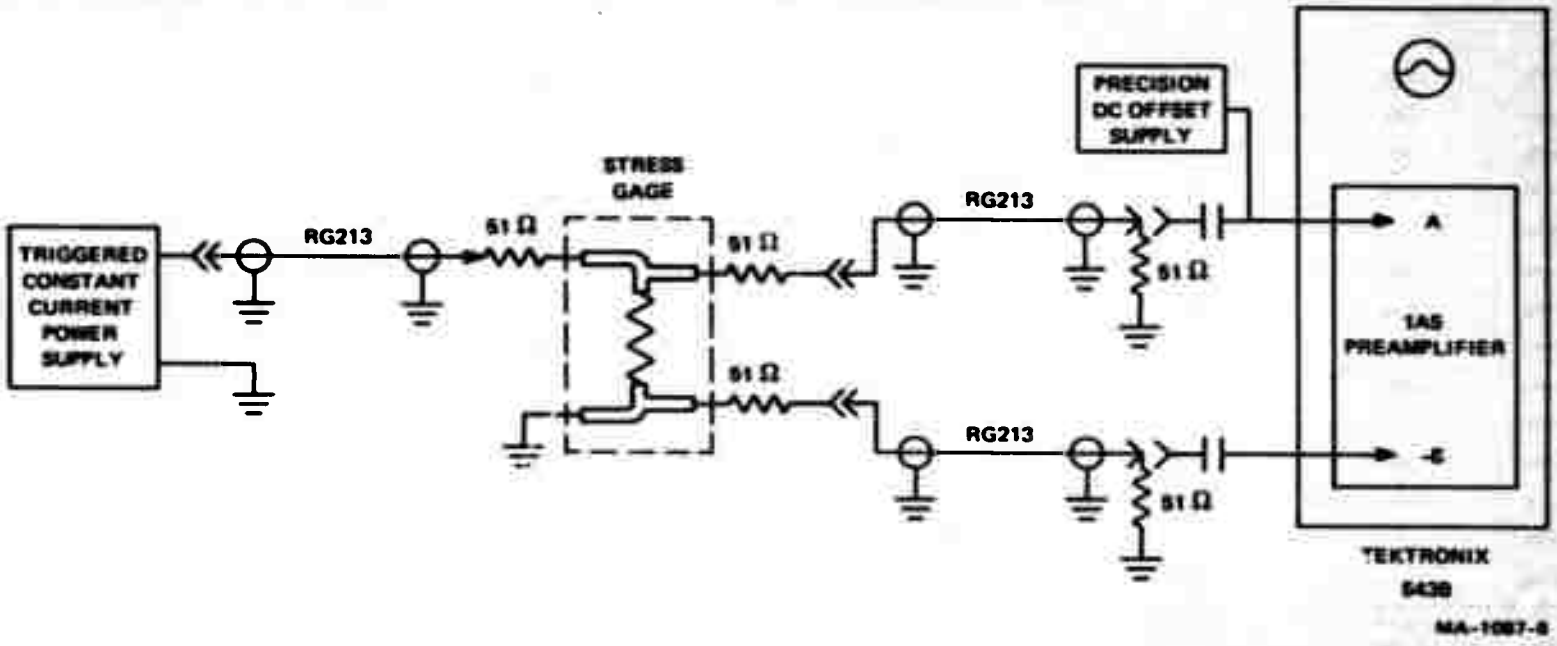

FIGURE 9 DIFFERENTIAL RECORDING SCHEME USED TO ELIMINATE NOISE FROM PIEZORESISTIVE SIGNALS

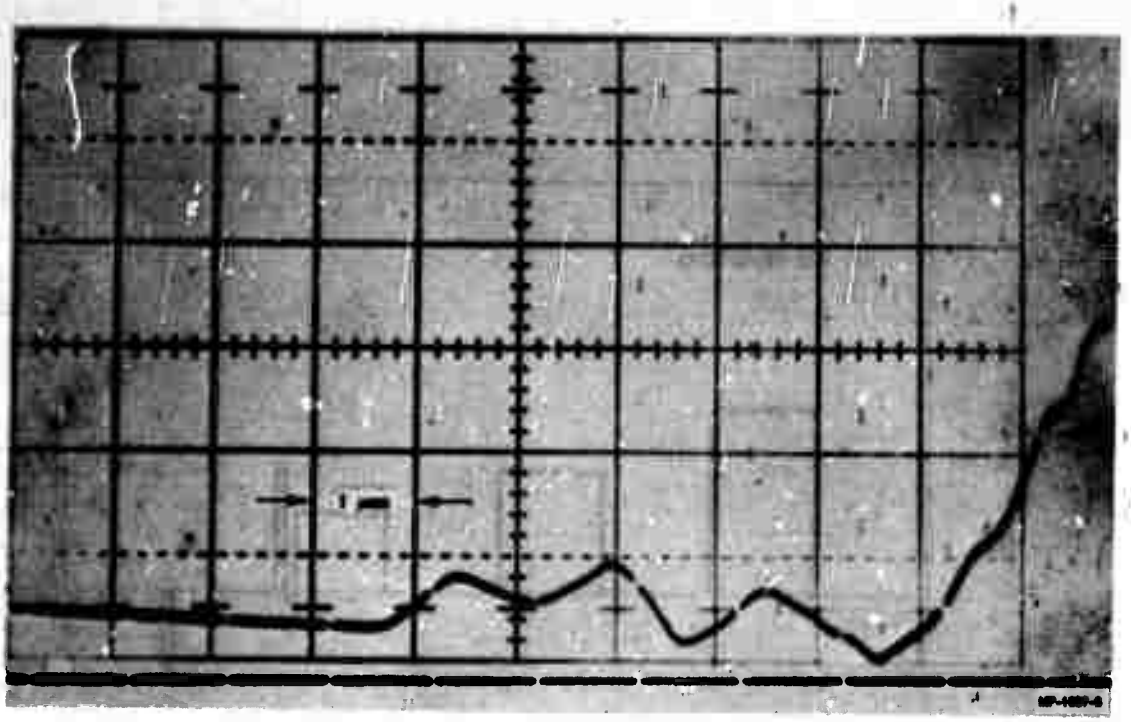

FIGURE 10 EXPERIMENTAL YTTERBIUM GAGE RECORD FOR SHOT 6

As can be deduced from the depicted stress history in Figure 7 the gage record for a specimen which does not undergo spall fracture should consist of three peaks followed by an anomalous stretching signal as the gage fails in tension. Thus the peaks recorded for Shot 6, Figure 10, indicate that no spall fracture occurred, a conclusion which was verified by sectioning the specimen and finding no cracks. Figure 11a shows the gage record predicted by a simple computer code for the case when no fracture occurs. The constitutive relation assumed is that for an ideally elastic solid. The stress-time profile is similar to the experimental record of Figure 10; the slopes and rounding of the experimental record are caused by tilt (one part of the gage sees the peak stress before another part), and by inelastic material response. According to our present calibration[35] the peaks on the record correspond to 80, 100, and 80 kg/cm^2 in the plexiglass backing material. The calculated peaks are 140, 90, and 60 kg/cm^2. The experimental peaks are spaced 1.5 μsec apart, in good agreement with 1.6 μsec for the computed peaks.

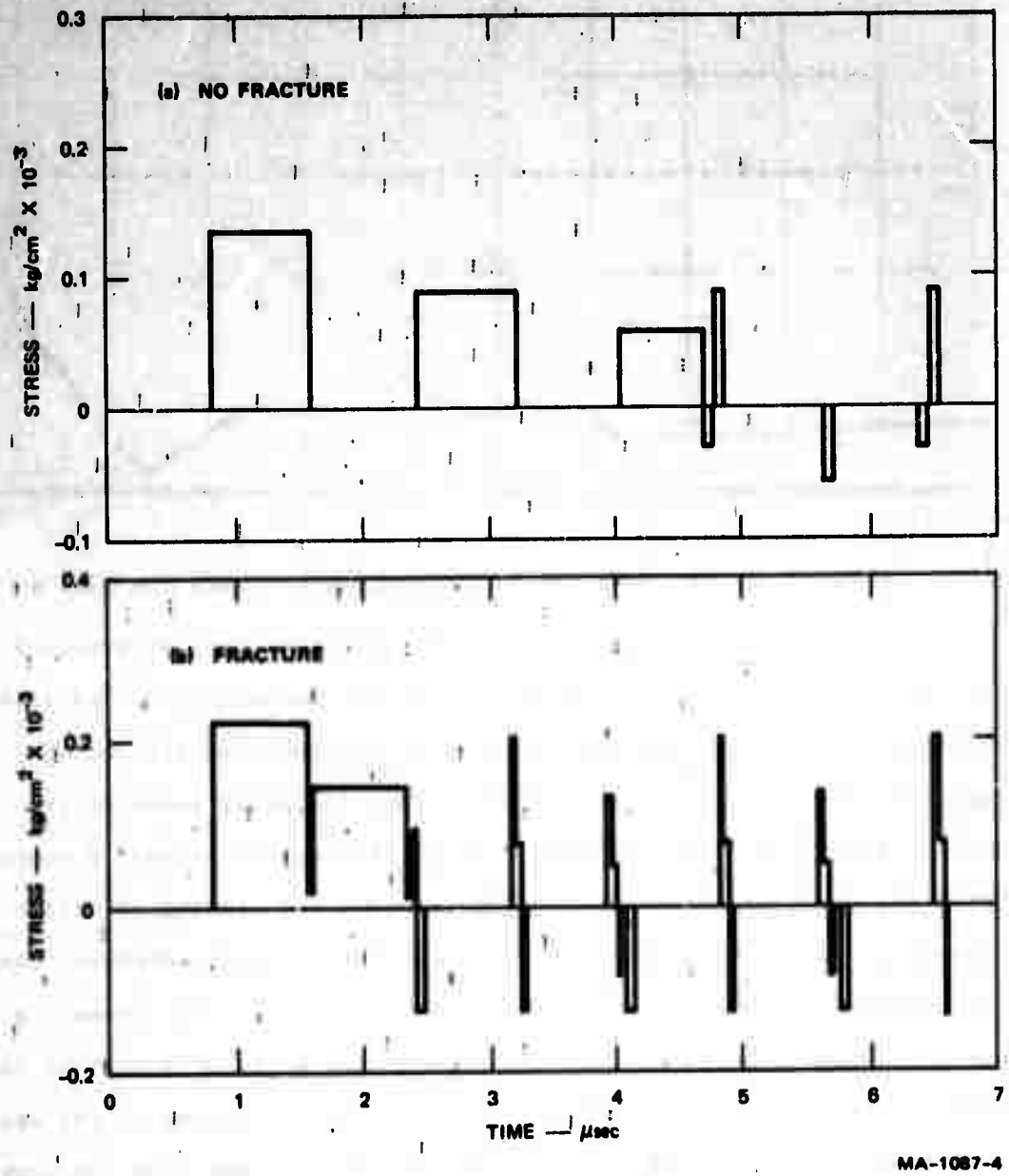

FIGURE 11 COMPUTER PREDICTION FOR SHOT 6 WITH NO SPALL AND FOR SHOT 4 WITH SPALL

Shot 11 at about the same stress in novaculite gave a record (Figure 12) similar to that for shot 6. The three peaks correspond to 150, 220, and 120 kg/cm^2, respectively, in plexiglass. However, the peaks are separated by 2.7 μsec. No spall cracks were found in this specimen, although it was damaged by radial cracks (see Figure 21).

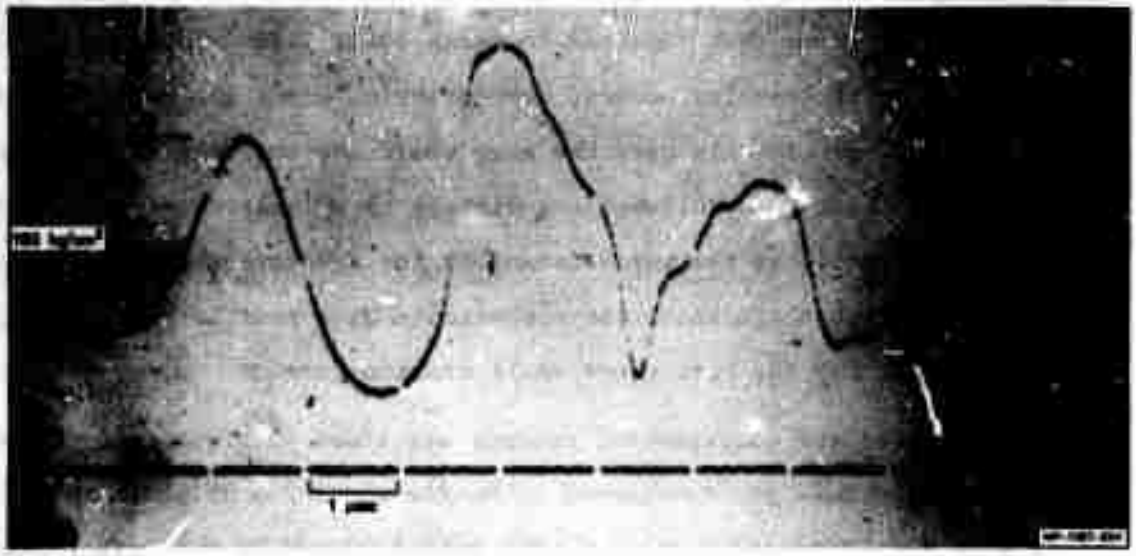

FIGURE 12 YTTERBIUM STRESS GAGE RECORD FOR SHOT 11

Shot 12 was impacted at higher velocity than Shot 11 and should have experienced a peak tension of about 520 kg/cm^2. The gage record shows a jagged peak too high in amplitude and too broad in time. Once again, no distinct spall cracks were found, but the specimen was seriously damaged by radial cracking. (See discussion on origin of radial cracks later in this section.)

At this point we decided that we would have to reduce the radial cracking to make meaningful measurements of the fracture strength. Several experiments indicated that thicker aluminum retaining rings or specimens having a larger diameter-to-thickness ratio would keep the novaculite specimen in one-dimensional compression long enough to prevent radial cracking from release waves originating at the outer ring boundary. The shock impedance of aluminum matches that of the novaculite closely, so we did not expect difficulties at the interface.

The next series of experiments with gages (Shots 15-23) were conducted on the 4-inch gas gun with specimens 1.0 or 1.25 inch in diameter and 0.3 inch thick. These had aluminum retaining rings with 0.6-inch wall thickness and 8^{o} taper. Our main goal in these experiments was to record the spall signal. Consequently all the tests were at projectile velocities considerably above that required to cause spall fracturing.

When spall cracking occurs, recompression waves are emitted as the cracks open up. In this case the gage would see the initial compressive pulse from the impact followed immediately by a lower compressive pulse, the spall signal, as the waves formed by the fracturing material reach the gage. Figure 11b shows the approximate wave profile predicted by the computer for the case where spall cracking occurs.

Seven of the experimental records are shown in Figures 13 through 19. The best of these are considered to be for shots 15, 17, 22, and 23. There is a general tendency to have a main peak followed by two lesser peaks, which we interpret as spall signals. For Shots 15, 17, and 22 the lesser peaks occur at about 1.6 and 2.5 μsec after the main peak.

For Shot 15 (Figure 13) the amplitude of the first peak corresponds to 530 kg/cm^2 in plexiglass, while the peak stress calculated from the impact velocity is 1070 kg/cm^2 in novaculite and 370 kg/cm^2 in plexiglass. The amplitudes of the two following peaks, each measured from its foregoing trough, correspond to 380 and 440 kg/cm^2 in novaculite, in good agreement with the measured dynamic tensile strength of novaculite reported in the next subsection.

The record for Shot 16 (Figure 14) is noisy and the signal arrived 13 μsec later than expected. A smaller peak does, however, follow the main peak and may be a spall signal.

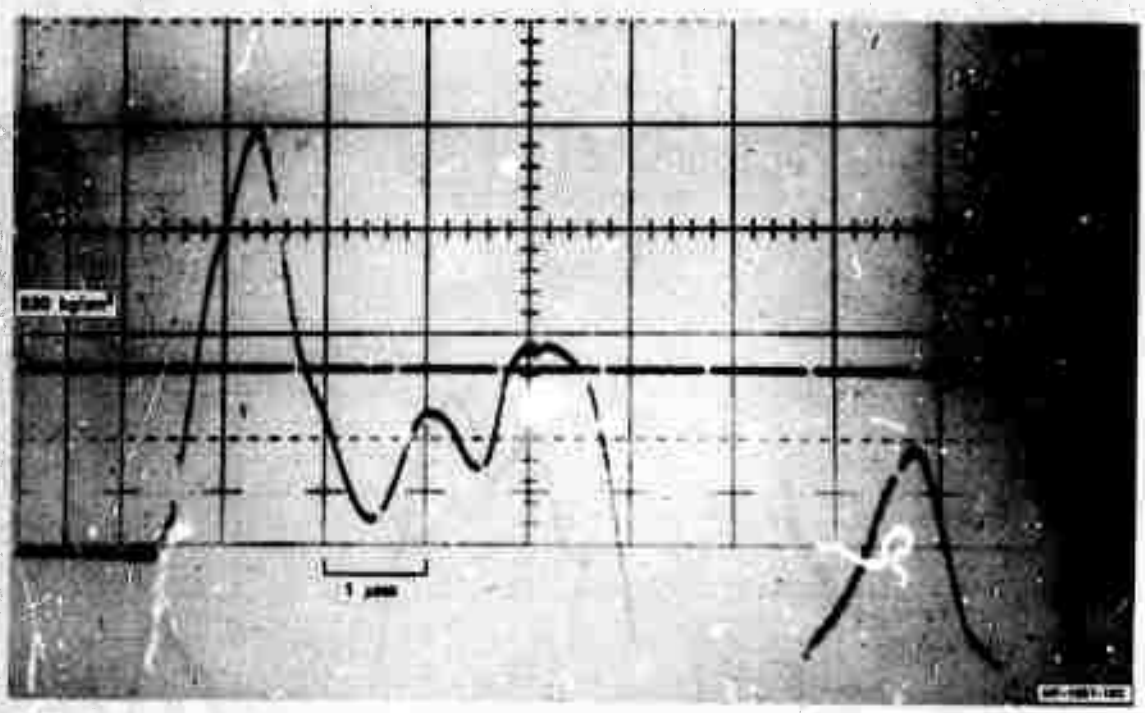

FIGURE 13 YTTERBIUM STRESS GAGE RECORD FOR SHOT 15

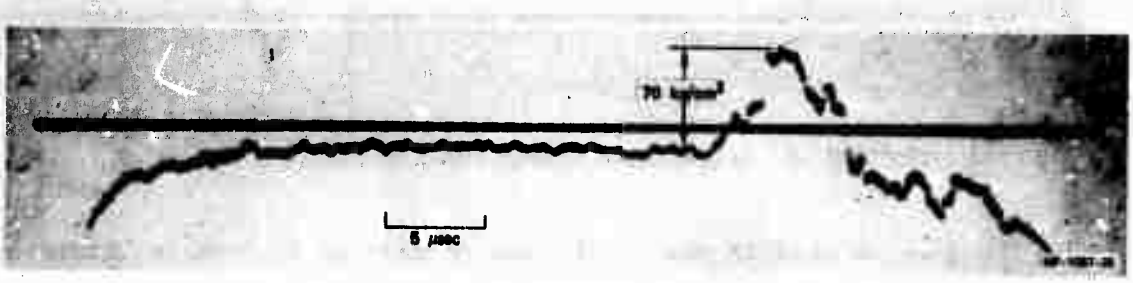

FIGURE 14 YTTERBIUM STRESS GAGE RECORD FOR SHOT 16

The record for Shot 17 (Figure 15) is similar to that for Shot 15. The main peak appears too high (560 kg/cm^2 in plexiglass, while calculation from impact velocity gives 320 kg/cm^2 in plexiglass), but the two following peaks appear reasonable and indicate 290 and 200 kg/cm^2 in novaculite, measuring from the foregoing trough to the peak in each case.

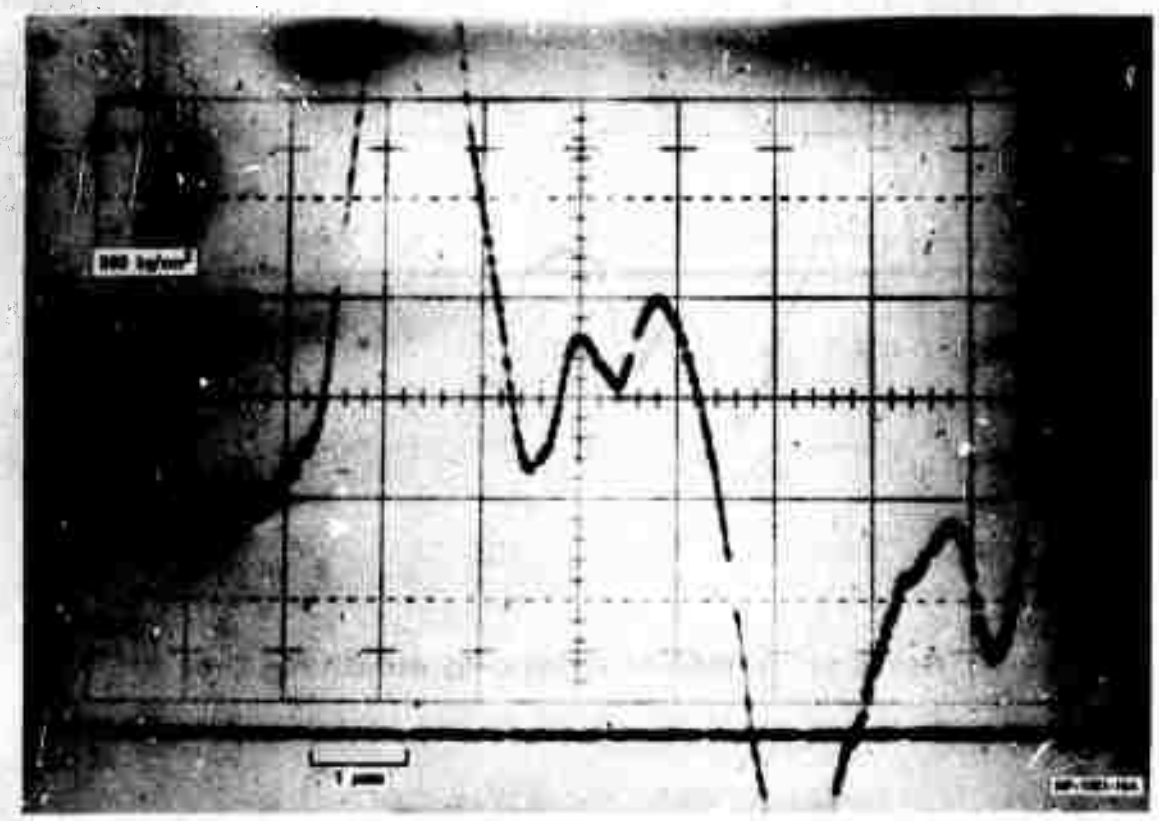

FIGURE 15 YTTERBIUM STRESS GAGE RECORD FOR SHOT 17

The gage in Shot 18 was noisy, and we made no attempt to interpret the record. In Shot 19 no record was obtained because the oscilloscope did not trigger. The record for Shot 20 (Figure 16) appears smeared out. The main peak corresponds to 240 kg/cm^2 in plexiglass, the peak stress in plexiglass calculated from impact velocity is 300 kg/cm^2. The plateau beginning at 1.1 μsec after the main peak and the high peak 3 μsec after the main peak may be spall signals. The latter would correspond to 660 kg/cm^2 in novaculite.

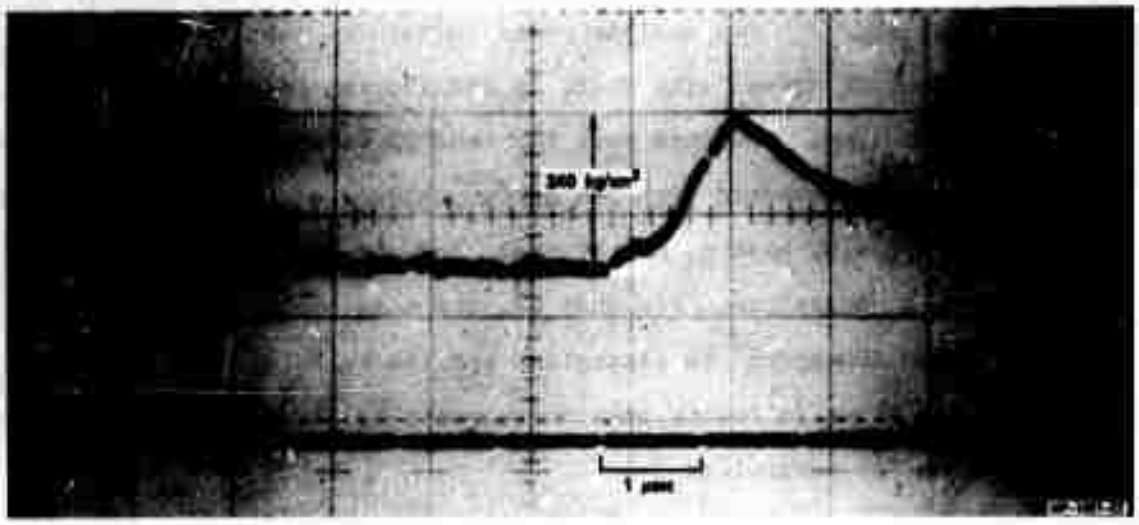

FIGURE 16 YTTERBIUM STRESS GAGE RECORD FOR SHOT 20

The record for Shot 21 (Figure 17) is similar to that of Shot 20, except that the amplitude of the main peak is very low, 70 kg/cm^2 in plexiglass as compared with the calculated value of 330 kg/cm^2. The same sort of plateau, sharp trough, and major rise follow the main peak as in Shot 20.

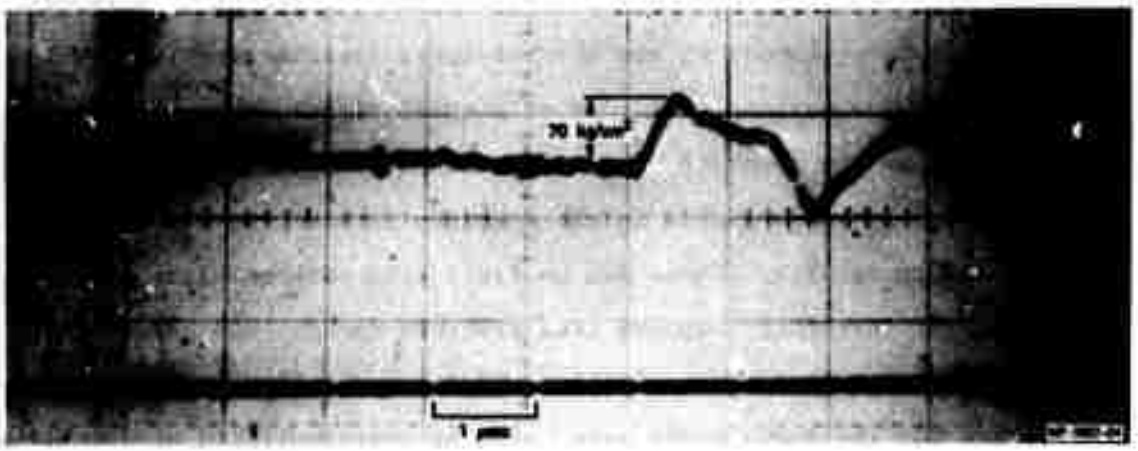

FIGURE 17 YTTERBIUM STRESS GAGE RECORD FOR SHOT 21

The records for Shots 22 and 23 (Figures 18 and 19) are more like those for Shots 15 and 17. Two smaller peaks follow the main one. The timing of the peaks for Shot 22 agrees with Shots 15 and 17; the peaks in Shot 23 are more spread out in time. The main peak for Shot 22 corresponds to 420 kg/cm^2 in plexiglass as compared with 330 kg/cm^2 calculated from impact velocity. The first following peak is nearly flat, and the second corresponds to 270 kg/cm^2 in novaculite. For Shot 23, the main peaks agree well; the gage recorded 290 kg/cm^2 in plexiglass and the calculated peak is 270 kg/cm^2. The first following peak corresponds to 150 kg/cm^2 and the second to 420 kg/cm^2 in novaculite.

In summary, the gage records clearly show the difference between the stress profile when no spall occurred, such as Shot 6, and the profile with spall, such as Shot 15. A number of difficulties were experienced in obtaining good records. Most of these, we feel, were technique development problems that have been overcome. We are now confident that the gage is recording the stress profile with fair accuracy. However, the profile is complicated because the fracture process itself is complicated. A number of spall cracks are activated, propagate, and coalesce. Instead of a single spall signal, which would be expected if a single spall crack were formed, we see several spall signals superimposed on each other. The maximum amplitude of a spall signal on good records corresponds to the fracture strength, as expected. In future experiments, with our recent improvements in the specimen release, we expect more interpretable results. Shots can be fired with peak stresses closer to the spall threshold, causing less fracture damage, and consequently generating a simpler stress profile. Furthermore, the computed stress histories for the above shots were based on oversimplified constitutive relations that did not contain stress relaxation caused by the developing damage. Computations with more sophisticated constitutive relations are presently underway.

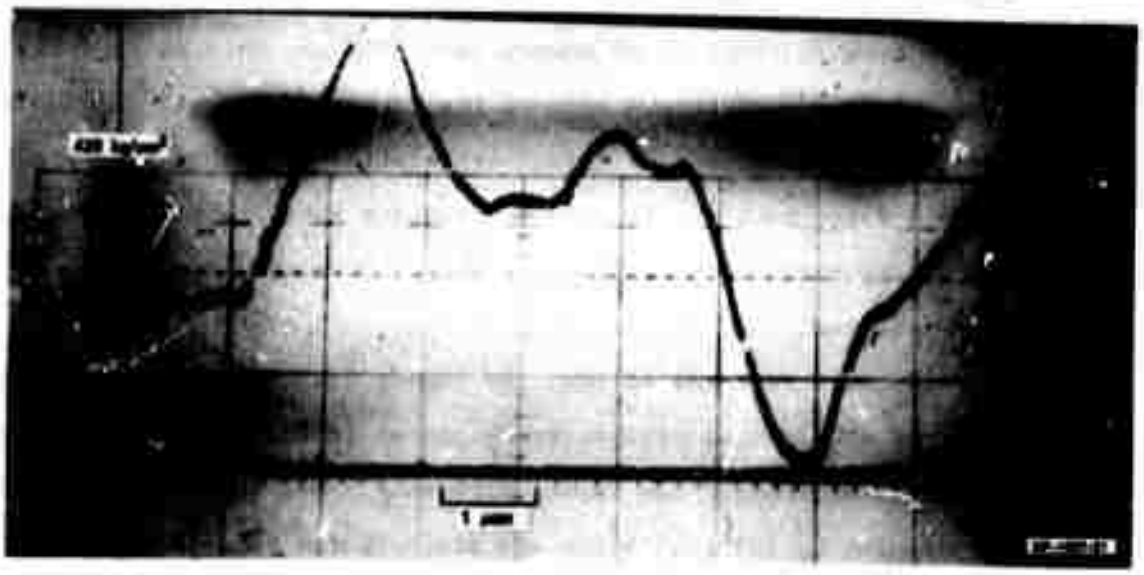

FIGURE 18 YTTERBIUM STRESS GAGE RECORD FOR SHOT 22

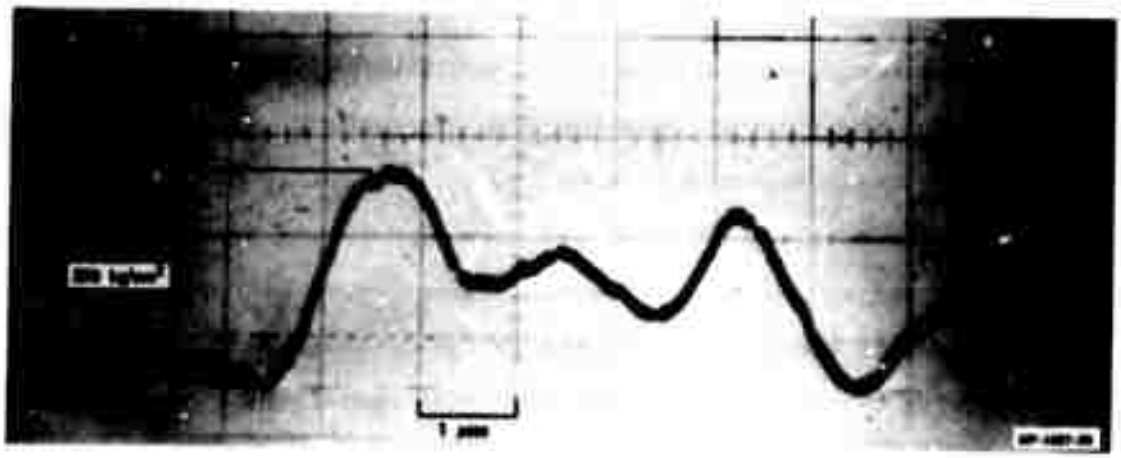

FIGURE 19 YTTERBIUM STRESS GAGE RECORD FOR SHOT 23

Uninstrumented Experiments

A series of 20 uninstrumented experiments was performed to measure the dynamic tensile strength of novaculite. The two main goals were to determine the effect of strain rate on the fracture strength of novaculite and to determine the effect of defect orientation on the dynamic fracture strength. A third goal was to produce fracture surfaces for examination in the scanning electron microscope to gain information concerning the fracture mechanism.

Ten specimens were cut so that the impact direction was normal to the planes of the initial cracks; crack planes in the remaining ten were oriented so as to contain the impact direction. All specimens were 1/2 inch in diameter by 1/4 inch thick and press-fitted into 1-1/2-inch diameter by 1/4-inch aluminum annuli. The outer periphery of each annulus was provided with an 8^{o} taper to facilitate ejection upon impact of the specimen-ring assembly from the aluminum target plate.

Very extensive cracking, usually resulting in blow-out of one or both sides of the specimen from the aluminum annulus, was produced in all of the first nine experiments even at stresses as low as 200 kg/cm^2. This initially puzzling behavior was prevented in the subsequent 11 shots by lightly tacking the tapered annuli to the target plates in three or four places with epoxy, as explained in the next section, instead of press-fitting. In the latter experiments no radial cracking occurred, and a good estimate of the dynamic fracture strength was obtained.

The results of this series of experiments are presented in Table III. The dynamic tensile strength was taken as the average of the highest stress at which no damage could be observed on diametrical sections of the specimen, and the lowest stress at which incipient spallation occurred. A cross sectional view of incipient spallation is provided in Figure 20. For the parallel specimen orientation, specimen 36 did not crack at 402 kg/cm^2, but specimen 35 did crack at 444 kg/cm^2; for the normal specimen orientation,

Table III

UNINSTRUMENTED DYNAMIC TENSILE EXPERIMENTS

Experiment No.	Specimen Orientation[a]	Impact Velocity (m/sec)	Maximum Peak Tensile Stress[b] (kg/cm^2)	Extent of Damage
24	P	26.8	748	Free surface blown out; thin rock layer at impact surface.
25	P	22.1	617	Free surface blown out; impact surface intact.
26	P	16.9	472	Specimen intact but badly cracked.
27	P	17.7	494	Free surface blown out.
28	P	14.6	407	Impact surface blown out.
29	P	12.5	349	Both surfaces blown out; piece remains in center of ring.
30	P	7.41	207	Free surface blown out.
31	P	11.1	310	Both surfaces blown out.
32	P	14.0	391	Both surfaces blown out; lens shaped section remains in ring.
33	P	12.2	340	No damage.
34	N	12.0	335	No damage.
35	P	15.9	444	1 spall crack about half specimen diameter.
36	P	14.4	402	No damage.
37	N	15.6	435	4 spall cracks on sectioned surface.
38	N	18.5	516	2 spall cracks on sectioned surface.
39	N	23.4	653	3 spall cracks on sectioned surface.
40	N	18.0	502	1 spall crack on sectioned surface.
41	N	16.8	469	No damage.
42	N	17.0	474	1 spall crack.
43	N	14.2	396	No damage.

Note: The tapered Al annuli were press-fit into the target plates for experiments 24 through 32. In experiments 33 through 43 the annuli were held lightly in place with four dabs of epoxy. Only the latter experiments provided meaningful dynamic fracture strength values.

a. P = specimen orientation was such that cracks preexisting in the rock lay roughly parallel to the impact direction.
N = specimen orientation was such that cracks preexisting in the rock lay normal to the impact direction.

b. Calculated from the measured impact velocity as described in the Appendix $\frac{\Delta\sigma}{\sigma} \simeq 4\%$.

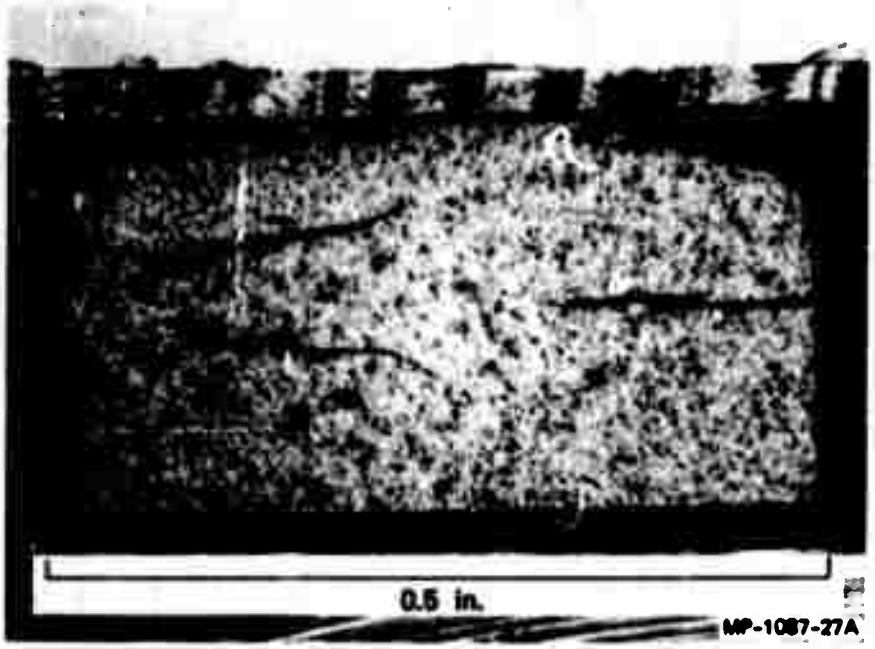

FIGURE 20 CROSS SECTIONAL VIEW OF SPECIMEN 39 SHOWING INCIPIENT SPALLATION

no cracking was observed in specimen 43, which was subjected to a peak tensile stress of 396 kg/cm^2, whereas specimen 37 showed cracking at 435 kg/cm^2. Thus the dynamic tensile strength of novaculite in the direction normal to the planes of inherent cracks is 415 ± 20 kg/cm^2; the dynamic strength in the transverse direction is 423 ± 20 kg/cm^2. We conclude that the dynamic tensile strength of Arkansas novaculite is insensitive to the orientation of preexisting flaws. In view of th pronounced crack orientation anisotropy of novaculite, the fracture strength isotropy was surprising. The probable explanation, however, is that the tips of preexisting intergranular flaws lie at high angles to the resultant macroscopic fracture plane and are equally difficult to activate in the two orientations. It should be borne in mind that the stress state is one of uniaxial strain, and thus triaxial tension. This means that the stresses in the two perpendicular directions normal to the impact direction are nearly as large as the impact stress.

The strain rate of the dynamic tests was estimated from the oscilloscope records of the ytterbium stress gages in the instrumented experiments described above. The rise time of the stress pulse is about a tenth of a microsecond, the elastic strain is about 7×10^{-4}, hence the strain rate is estimated to have been approximately 7×10^{3} sec^{-1}, since this is more than seven orders of magnitude higher than the strain rates of the quasi-static ring tests, the negligible difference in strength values indicates that the fracture strength is also strain-rate insensitive, at least in this range.[a]

Origin of Radial Cracks

In the early stages of this work specimens subjected to dynamic tensile loading in the gas guns were observed to have fractured in a radial mode in addition to the planned spallation mode. Under conditions of flat plate impact, the cylindrical rock specimens were expected to fail by propagation of so-called spall cracks roughly normal to the impact direction. It was therefore somewhat surprising to consistently observe a radial network of cracks parallel to the impact direction and extending from the impact side into about the midplane of the specimen. Figure 21 is a photograph of the radial network of cracks on the impact surface of a specimen, and Figure 22 is a diametrical section showing the depth to which the cracks extend into the interior.

Such radial cracks were undesirable since they complicated the failure process and made interpretation of stress gage records uncertain. The reason for their occurrence was elusive. We first speculated that rarefaction waves running in from the specimen periphery were responsible

---

[a] In light of experimental results by Rinehart[36] on limestone and marble at strain rates exceeding 10^{7} sec^{-1}, it is conceivable that novaculite could show rate sensitivity at higher strain rates.

FIGURE 21 RADIAL CRACKING PATTERN ON THE IMPACT SURFACE OF NOVACULITE

for radial cracking, so in attempting to eliminate them, specimens were inserted into thick aluminum annuli. Since the shock impedance of aluminum is similar to that of novaculite, this alteration had the effect of displacing the specimen periphery so that the tensile pulse producing the spall cracks was completed before the rarefaction waves could reach the specimen interior. An equivalent measure taken to eliminate radial mode cracking was to perform experiments in a larger bore gas gun, using larger specimens.

Several experiments using this technique were successful in that spall cracks but no radial cracks were produced. In other cases, however, the converse was true, and it was obvious that the problem was not solved.

FIGURE 22 CROSS SECTIONAL VIEW OF A SPECIMEN SHOWING RADIAL CRACKS EXTENDING INTO ABOUT THE MIDPLANE

During the course of carrying out the series of uninstrumented recovery shots, an observation was made that indicated the solution. An impacted specimen was not ejected into the catcher tank, but rather remained in the target plate. Radial cracking was significant and suggested that the press fitting prevented the specimen from immediately popping free under the low impact velocities, and the ejection delay permitted bending waves to produce the radial cracks. To test this theory, specimens were weakly held in the target plate with a dab of epoxy in several places. This technique was used for the last 11 specimens with complete success; i.e., no radial cracking occurred in any of these experiments (see for example, Figure 20).

IV THE MECHANISM OF FRACTURE

Fractographic Observations

The fracture damage produced during most of the impact experiments consisted of many cracks in essentially two main orientations: cracks lying perpendicular to the impact direction (generally referred to as spall cracks) and unexpected cracks whose planes roughly contained the impact direction. The spurious radial cracks that occurred because the specimens were held too tightly in the target plate were eliminated in later experiments as explained in the previous section, and thus an unambiguous fractographic analysis could be performed on the spall cracks.

Fractography of specimens that remained intact after impact was performed by sectioning the specimens on a diameter, polishing the surface of section, and examining the fracture pattern by means of optical microscopy. At low stresses just slightly in excess of the dynamic fracture strength, only a few spall cracks (usually less than four intersected the surface of section) were formed (Figure 20), but these were usually large, extending typically to about a third of the specimen diameter. Some evidence of crack branching was observed, indicating that propagation velocities were high,probably approaching a limiting crack velocity. The low number of cracks was expected at these stresses, since only the largest or near largest cracks could be activated. Furthermore, the stress quenching effect in the volume around the rapidly running cracks would tend to prevent additional near-critical cracks from being activated during the tensile pulse.

At higher stresses, say 50% in excess of the dynamic tensile strength, considerably more inherent cracks were activated. Probably growing at near limiting velocities, these cracks, because of their high number density, soon grew into each other, and the fracture process proceeded

to the next stage--coalescence. Figure 23 is a photograph of a polished cross section showing coalesced cracks and incipient fragmentation. Individual cracks have joined up, and in doing so, have produced a network of weakly held unfractured rock fragments, Ths missing half of the specimen in Figure 23 has undergone complete fragmentation, and the individual fragments have fallen out of the restraining ring.

The fracture surfaces of spalled and fragmented novaculite specimens were examined by optical and scanning electron microscopy. The purpose was to look for inhomogeneities, which could have served as crack activation sites, and such crack growth markings as river lines and hesitation bands, all of which would provide clues concerning the fracture mechanism.

As is typical of most rocks, the fracture surfaces were nearly featureless and yielded scant evidence of how failure occurred. The broken surfaces consisted of countless, well-defined, equisized polygonal blocks--quartz grains exposed by the passage of a crack along the grain boundaries, as illustrated by the background structure in Figure 24. Thus the measured fracture strength is really the strength of the "cement" holding individual grains together, and not of the quartz itself. No obvious defects could be found where cracks had nucleated, and no telltale lines such as often mark the boundaries of preexisting flaws in other materials when activated under a tensile pulse were evident. Although no fracture markings could be found to confirm it, it is likely that anomalously large grains such as that shown in Figure 24 served as activation sites.

It was possible on occasion to identify propagation markings and hesitation lines on fracture surfaces, Figure 25, which suggest that cracks expand radially outward from their activation sites on planes normal to the tensile direction. This crack propagation mode was found to operate in polymers,[22] Figure 26, under similar dynamic loading conditions.

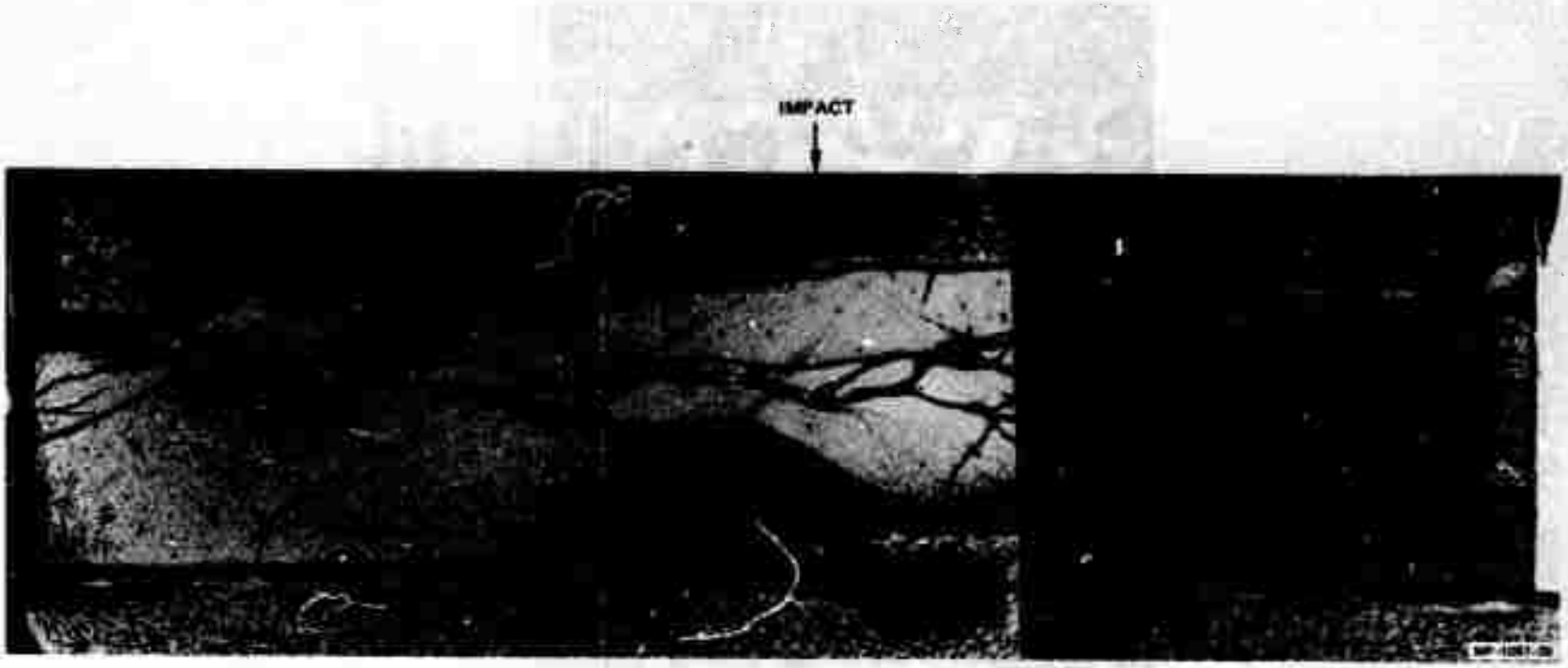

FIGURE 23 CROSS SECTIONAL VIEW OF SPECIMEN 21 SHOWING THE CRACK COALESCENCE BEHAVIOR AT A STRESS LEVEL 50% HIGHER THAN THE DYNAMIC FRACTURE STRENGTH

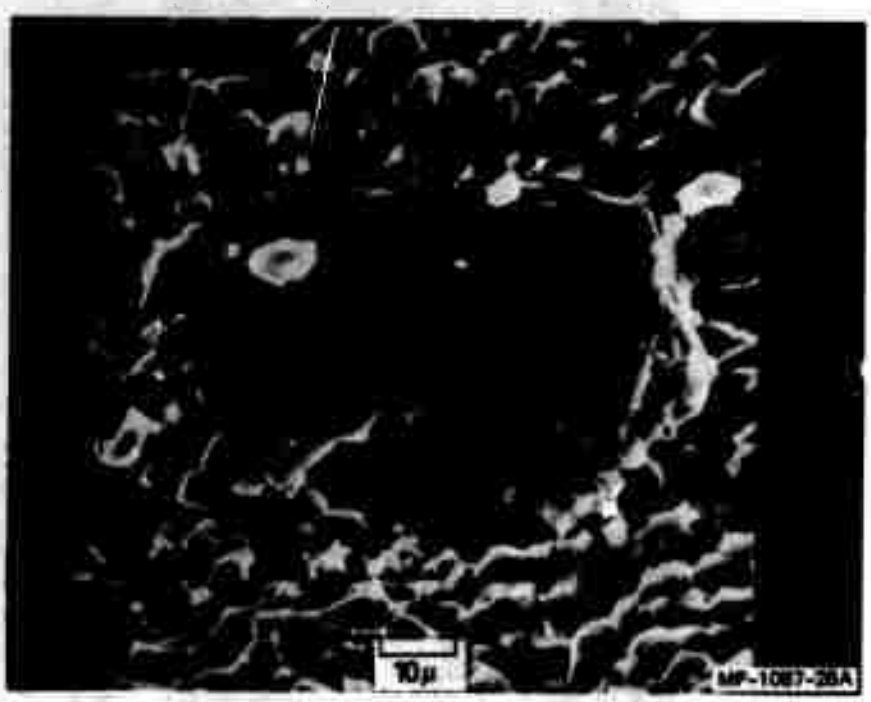

FIGURE 24 ELECTRON MICROGRAPH OF A LARGE QUARTZ GRAIN, FOUND ON THE FRACTURE SURFACE OF AN IMPACTED SPECIMEN, THAT MAY HAVE SERVED AS A SPALL CRACK NUCLEATION SITE

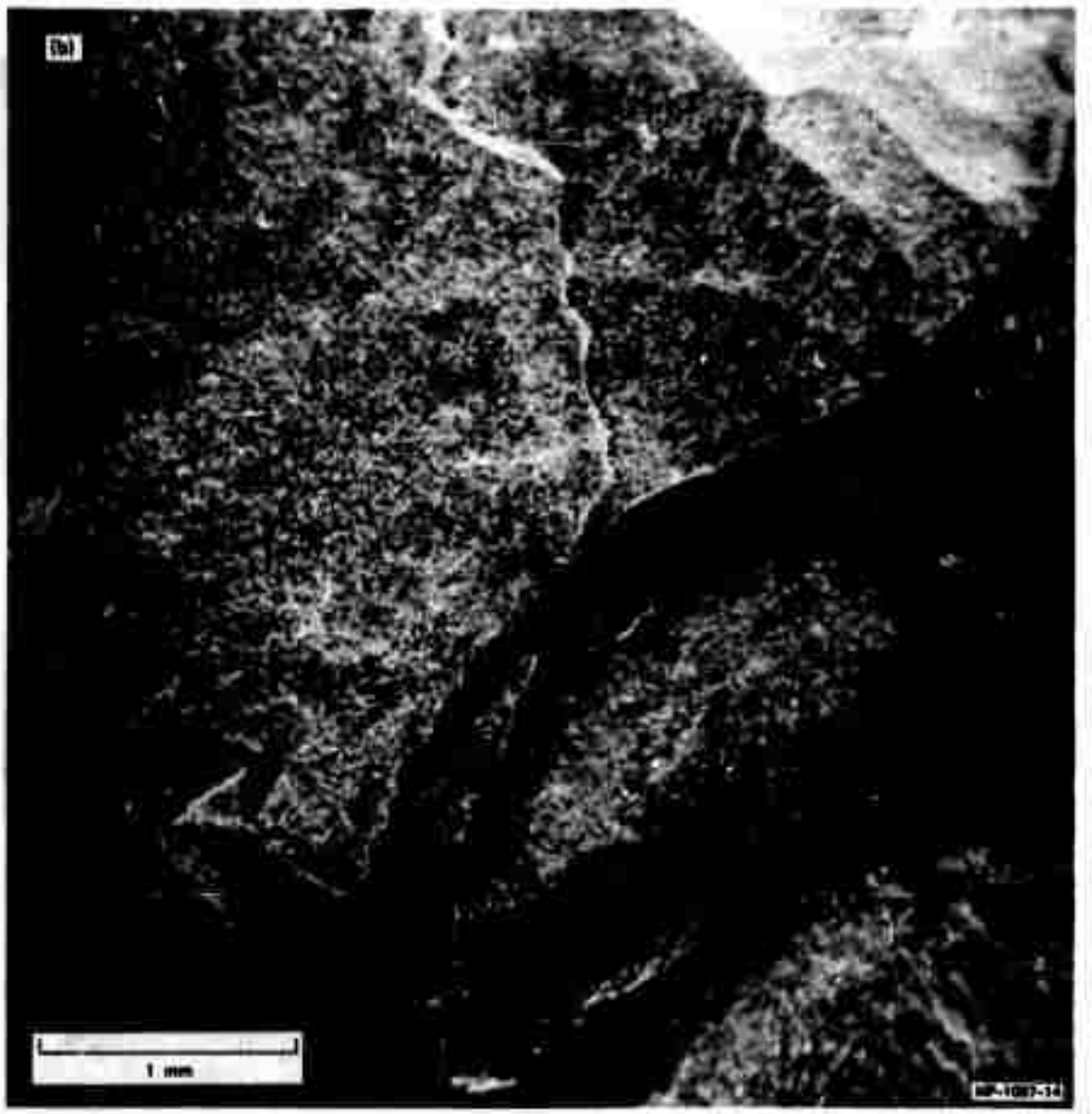

FIGURE 25a SECTION OF CIRCULAR HESITATION LINE ON THE FRACTURE SURFACE OF DYNAMICALLY LOADED NOVACULITE

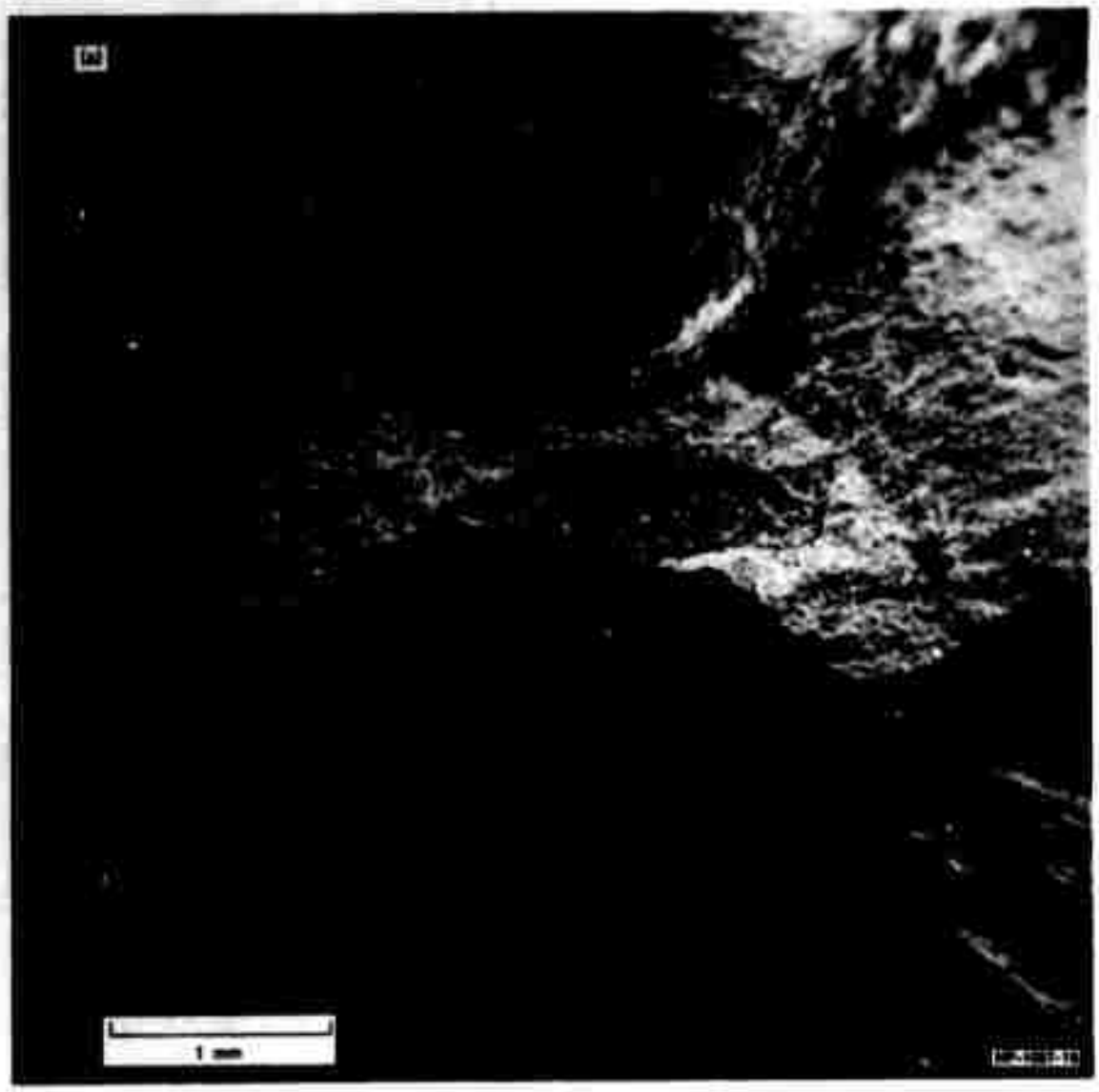

FIGURE 25b SECTION OF CIRCULAR HESITATION LINE ON THE FRACTURE SURFACE OF DYNAMICALLY LOADED NOVACULITE

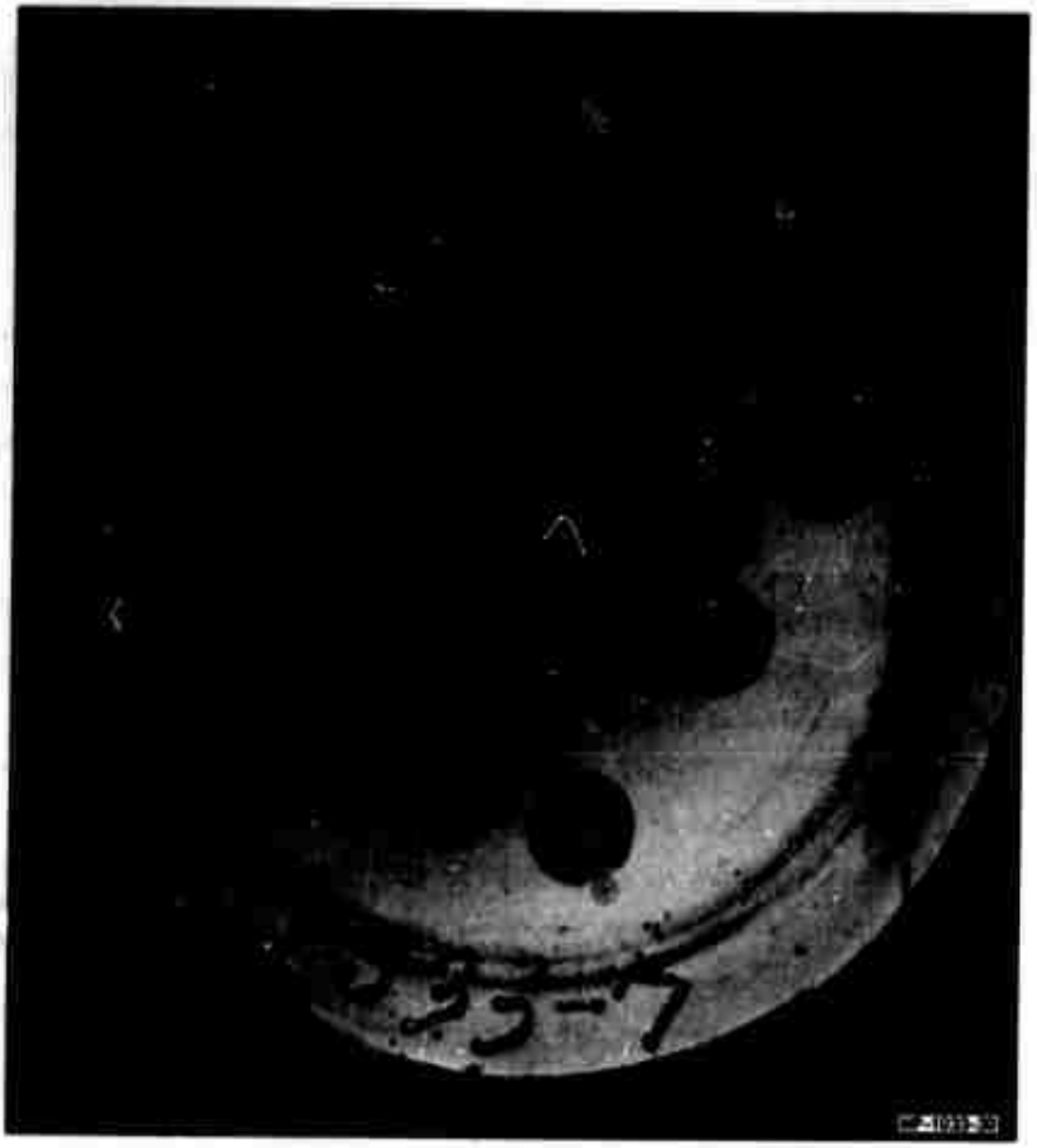

FIGURE 26 INTERNAL CRACKS IN POLYCARBONATE PRODUCED BY A SHORT-LIVED TENSILE PULSE

Fracture Mechanism in Novaculite Under a Short Tensile Pulse

On the basis of these fractographic observations and previous observations carried out on a transparent polymer, we propose that fracture in rocks under high rate loading occurs in the four stages described below.

1. Simultaneous activation of a number of preexisting structural defects--These include channel-like pores, large voids, planar fissures, and grain boundary seams (see Section III). Since the stress required to activate a flaw decreases with increasing flaw size and decreasing root radius of the crack periphery, the largest and sharpest flaws are expected to be the most influential in instigating the fracture process. However, in the case of novaculite, the dynamic strength was found to be independent of the orientation of the large plate-like flaws, indicating that the randomly oriented grain boundary flaws may control internal spall initiation.

2. Growth of the activated flaws radially outward--Circular hesitation lines on fracture surfaces of impact loaded novaculite, Figure 25, suggest that penny-shaped cracks grew by radial expansion. This conclusion is supported by similar impact experiments[22] on a transparent plastic where individual cracks could be directly observed, Figure 26. The path of the fracture is determined by two factors: the direction of the maximum tensile stress and the local structural discontinuities in the vicinity of the crack periphery. Strain energy release per unit crack advancement is greatest for crack extension normal to the direction of maximum tension. This tends to maintain crack growth on a level plane since the stress pulse in these experiments is constant in direction. The absence of smooth planar cracks in novaculite is a result of the micro and defect structure. Since the strength of the quartz grains is greater than the strength of the bonding between them, the microstructure

determines the small scale roughness of the fracture path, because the advancing crack must pass around the grains rather than through them. In a similar manner the defect structure causes both small and large scale deviation from the planar fracture path favored by the maximum tensile stress. The crack intersects inherent pores, fissures, and voids as it grows, and incorporates these into the crack. Such flaws do not generally lie in the tensile plane, however, and thus result in larger scale irregularity of the fracture surface. Moreover, since the crack prefers to follow a least-resistance path, it is not even necessary that structural discontinuities intersect the plane of preferred propagation; rather it is often sufficient when a large flaw lies somewhat out of the preferred plane, for an interaction of the stress fields can cause the crack to turn into the flaw. Considerable roughness also results from a splitting-up of the main crack into two or more branches as a consequence of the defect structure or of high fracture speeds. Secondary branches may run a distance and stop, or they may join up with other cracks, which sometimes produces free chips of material. Crack branching is responsible for the shattering phenomenon in brittle materials under quasi static loading.

The fracture path then is determined not simply by the direction of the maximum tensile stress σ_{max}, but rather by the ratio of σ_{max} to the local strength of the material S_{loc}. Fracture propagation occurs on those planes that are normal to the direction in which σ_{max}/S_{loc} is a maximum. Notice that since S_{loc} varies strongly with position in the material, the fracture path will not be constant but will wander haphazardly through the specimen along the course of least resistance.

3. Coalescence of the expanding cracks--Two radially expanding cracks on nearby planes will eventually approach each other to the point where the concentrated stress fields associated with the crack tips overlap. The material between the two cracks is subjected to magnified

stresses, and because of the proximity of two free surfaces (in which the stress has fallen to zero), the maximum stress direction is altered. Accordingly, the direction of crack extension is altered, usually causing one or both cracks to turn in to one another. This process, carried to completion so that the two cracks join up, is called crack coalescence and is an important stage in the fracture process. Inability of cracks to coalesce would be manifested by a significant increase in the toughness of rocks. Coalescence accelerates fracture since crack size discontinuously increases, resulting in a sudden reduction in the available load-supporting area and a corresponding step-like reduction in the material strength. The cross-sectional area capable of bearing load diminishes at an ever-accelerating rate and leads to the final stage of fracture.

4. Fragmentation of the specimen--The connectivity of individual cracks on at least one fracture path is complete, and the cracks have run to the outer surfaces. Cracks on other planes stop growing because the stress is relieved. At stresses barely exceeding the fracture strength, the specimen may break into only two pieces, but at stresses considerably greater than the fracture strength, significant fragmentation occurs. The number of fragments produced is thought to be largely dependent on the applied stress and the size distribution of initial defects. Crack branching can also contribute to the fragmentation process.

V A COMPUTATIONAL MODEL FOR DYNAMIC FRACTURE OF ROCK

For computational purposes the tensile failure of rock is assumed to occur in four stages:

(1) Activation of a number of preexisting structural defects
(2) Propagation of activated cracks radially outward
(3) Coalescence and branching of propagating cracks
(4) Isolation of individual rock fragments from one another.

The important quantities to be determined are:

(1) The number of flaws that become running cracks
(2) The distance that each crack propagates
(3) The degree to which coalescence and branching occurs
(4) The size distribution of the resulting fragments.

It is assumed that these quantities are governed by three factors: the initial defect structure in the rock, the inherent fracture resistance of crack-free material, and the applied stress history. To predict the failure behavior of a rock, quantitative measures of these three factors must be obtained and related to the above listed quantities, which are then related to each other by means of a computational model.

During this year the first two stages were treated in some detail; the procedure for calculating these quantities and the results for novaculite are presented below. The latter two states will be treated in the course of the second year.

Stage 1: Flaw activation calculations for novaculite--We assume flaw activation to occur according to Griffith-Irwin fracture mechanics concepts,[2-4] i.e., flaws having a radius c larger than a certain size $c^* = c^*(\sigma)$ are activated by the applied stress σ, whereas smaller flaws are unaffected. Fractography showed that internal flaws control the activation stage of the fracture process. Of the various geometries for which fracture mechanics stress analyses exist, Sneddon's relation[30] for an internal penny-shaped crack in an infinite elastic medium subjected to a uniform tensile stress normal to the crack plane

$$c^* = \pi K_{Ic}^2 / 4\sigma^2 \qquad (7)$$

most nearly applies to the conditions of our experiments, i.e., the cracks are roughly penny-shaped, and the specimen behaves as if it were infinite during the life of the tensile pulse. Using this expression to relate the measured dynamic tensile strength to the half length of the largest flaw, we calculate the dynamic fracture toughness of novaculite to be about 110 $kg/cm^{3/2}$. Substituting this value into Eq. (7) we obtain the functional expression for relating the size of the smallest pre-existing defect which will be activated by an applied dynamic load of stress level σ

$$c^* \simeq 10^4/\sigma^2 \qquad (8)$$

To obtain the number of defects which will be activated by the applied stress, we must determine the size distribution of preexisting flaws in the rock sample and combine this information with Eq. (7). Perhaps the most reliable and convenient way to determine the size distribution of preexisting flaws is by sectioning the rock sample, counting and measuring the flaw traces on the section surface, and statistically transforming the data. Nine overlapping micrographs spanning the diameter of a rock specimen were assembled into a composite picture of the rock surface. The total area was slightly greater than 1.1 cm^2 and in this area 194 traces of preexisting flaws were observed, counted, and measured. We assumed that crack activation occurs most easily at the large plate-like flaws, although in light of the constancy of the dynamic fracture strength with specimen orientation we have not ruled out the possibility that grain boundary fissures may control the activation stage of the fracture process. The data were converted to obtain the size distribution per unit volume by means of a statistical transformation similar to that used by Scheil.[5,6] The procedure was implemented by a computer code.

The cumulative number density of flaws having half lengths greater than c as a function of c are presented in Figure 4 and is well described by the analytical form

$$N = \delta(c)\exp[11-(3.7 \times 10^2)c + (0.42 \times 10^4)c^2] \quad (4)$$

where

$$\delta(c) = 1 \quad \text{for} \quad 0 < c \leq 0.05$$

$$\delta(c) = 0 \quad \text{for} \quad c > 0.05$$

and c is in centimeters.

To obtain the number of flaws activsted N_{act} by an arbitrary dynamic stress σ, Eqs. (4) and (8) are combined,

$$N_{act} = \delta(\sigma)\exp[11 - (3.7 \times 10^6)/\sigma + (4.2 \times 10^{11})/\sigma^2] \quad (9)$$

Here

$$\delta(\sigma) = 1 \quad \text{when} \quad \sigma \geq 410 \text{ kg/cm}^2$$

and

$$\delta(\sigma) = 0 \quad \text{when} \quad \sigma < 410 \text{ kg/cm}^2$$

Stage 2: Crack propagation calculations for novaculite--The distance each crack can propagate depends on the crack velocity and the duration of the stress pulse. Ytterbium stress gages were used to measure the latter in this work and crack velocities were inferred from direct measurements of the distance propagated by cracks in essentially crack-free material. The radii of the cracks shown in Figure 20 are about 2 mm. The ytterbium stress gage records indicated that the stress duration was about one microsecond, in agreement with the result obtained from simple calculations using the measured elastic wave speed and the thicknesses of the specimen and flyer plate as depicted in Figure 7. Thus crack propagation velocities of 2×10^5 cm/sec are indicated--an interesting result, since it is approximately one-third of the measured

longitudinal wave velocity for novaculite, and is thus in agreement with theoretical estimates of the maximum crack velocities of brittle materials.[37-40] Materials such as Armco iron and beryllium, investigated in other projects,[15,41] fractured in a brittle manner at high strain rates, but exhibited viscous crack propagation and maximum crack speeds well below $c_\ell/3$. Knowing the crack propagation speed and that propagation occurs radially outward from activation sites, the fracture surface area produced per crack A_1 during the period of the stress pulse Δt can be approximated by

$$A_1 \tilde{=} 2\pi(c_\ell \Delta t/3)^2 \tag{10}$$

providing the crack was not stopped prematurely by barriers to crack growth or coalescence with other cracks. Thus for stresses only slightly greater than the dynamic tensile strength where significant crack coalescence does not occur, the total fracture area produced in novaculite by a stress pulse of known peak stress σ and duration Δt is given by

$$A_{total} = \frac{2N_{act}}{3}(c_\ell \Delta t)^2 \tag{11}$$

where c_ℓ is the longitudinal wave speed.

In Eqs. (10) and (11) we have neglected crack acceleration, assuming in essence that cracks reach the maximum speed $c_\ell/3$ in zero time. A solution of the Dulaney and Brace[39] formula confirms that the acceleration time is very short relative to the stress duration in this work and thus supports this assumption.

Thus Eq. (11) uses traditional fracture mechanics and simple elastic crack propagation theory to obtain a crude approximation of the fracture

damage produced in novaculite by a known stress history. To illustrate the method we consider a square tensile pulse 500 kg/cm^2 in amplitude and 0.8 microsecond in duration and calculate step-by-step the amount of fracture surface area which will result. According to Eq. (7) all preexisting flaws of half length greater than 0.04 cm will be activated. From the flaw size distribution curve Eq. (4), we calculate that there are about 20 flaws preexisting in the rock with half lengths greater than 0.04 cm and thus 20 cracks begin to propagate. Since a relatively low number density of cracks is activated, crack growth will continue until the stress vanishes (i.e., the growth distance is not shortened by coalescence) and the total fracture surface area produced is given by Eq. (11) to be 3.2 cm^2. Based on a qualitative estimate of the fracture damage in a specimen which had experienced a similar stress history, this estimate seems reasonable.

Finally it should be pointed out that the tensile loading phase experienced by a specimen which suffers fracture damage is not a simple square wave. The fracture damage as it develops modifies the tensile pulse continuously, for the individual cracks as they nucleate and grow emit recompression waves which propagate through the specimen and unload the material. Sophisticated computer codes which calculate crack acceleration, crack opening, and the stress histories in specimens undergoing fracture have been developed at SRI on other projects. We expect to make use of these codes as we further develop the model for dynamic fracture in rock.

Stage 3: Crack coalescence and crack branching--As radially expanding cracks on nearby planes approach each other, the magnified stress fields about the crack tips overlap and the maximum stress direction is altered. Since it is energetically most favorable for cracks to run normal to the direction of maximum tensile stress, the cracks turn into

each other, and join up. Fragments are produced when a sufficient number of cracks join up to form a continuous surface about an unfractured segment of material. Figure 23 is a photograph of a cross section of specimen 21 showing incipient in situ crack coalescence and fragmentation.

Another mechanism of fragmentation is by branching of individual cracks. Crack branching has long been observed in brittle materials and has been extensively studied in glass.[42] The phenomenon is believed to occur when the crack speed reaches the maximum velocity of about $c_\ell/3$. There is evidence of branching in novaculite in Figure 23. It is apparent how this phenomenon can contribute to fragmentation of the specimen.

Stage 4: Fragmentation--The duration of the stress pulse will influence the extent of fragmentation produced by either mechanism. In the present experiments stress durations of about a microsecond permitted cracks growing at near theoretical velocities in unfractured material to reach a diameter of about four millimeters. This means that at stress levels sufficient to activate about five preexisting cracks/cm^2 or more, fragmentation will occur.

The coalescence and fragmentation phases of the dynamic fracture model will receive considerable attention during the next year. In particular the fragment size distribution will be determined by direct measurement of loose fragments and possibly in intact specimens by a section and transform method similar to that used to obtain the pre-existing defect size distribution. These results will be correlated with the applied stress and stress duration to complete the predictive capability for novaculite.

VI PLANS FOR FUTURE WORK

The capability of controlling to some extent the particle size distribution produced by rock blasting would have obvious benefits. Two of the most important are: (1) more economical and efficient use of charges to excavate a given site and (2) production of fragment sizes most suitable for a given application or for easy handling. Some ideas on how to achieve such a capability have been developed during the course of this years work and are discussed in this section.

Three factors are important in determining the fragment size distribution resulting from dynamic loading of rock: the initial defect structure in the rock, the inherent fracture resistance of crack-free material, and the applied stress history. Only the last of these can be easily varied; quantitative measures of the first two factors must be obtained. During this first year convenient methods for determining initial crack size distributions and inherent fracture resistance of novaculite were developed, and stress histories were measured.

The first task in the second year will be to determine in novaculite the fragment size distributions which result from dynamic loads. This information will be correlated with the initial defect distribution, the inherent fracture resistance, and the measured stress history to complete the predictive capability for novaculite. Following this, we will begin to test the applicability of the model to other rocks.

The fragmentation experiments on novaculite will be performed with the gas guns at various stress levels significantly above the fracture strength to produce various degrees of specimen comminution. We will develop techniques to recover 100% of the fragmented specimens, and quantitatively determine the fragment size distribution by sieve analyses. We will also attempt to recover intact specimens in which large numbers of activated cracks have coalesced. Such specimens could be analyzed by fractographic examination of diametrical sections. Stress wave propagation

in novaculite will be calculated by computer codes, utilizing constitutive relations that include the effects of stress relaxation caused by developing fracture damage.

To verify and generalize the dynamic fracture model developed for novaculite, the dynamic fracture behavior of Sioux quartzite, Westerly granite and Tennessee marble will be studied. These rocks will be characterized with respect to static strength, defect and microstructure, inherent fracture resistance, and other properties influential to the fracture behavior. Dynamic tensile tests will be performed with the gas guns to obtain the dynamic fracture strength, the inherent fracture resistance under high rate loading, and the strain rate sensitivity. Tests on both wet and dry specimens of Westerly granite will be made. Ytterbium stress gages will be used to monitor stress histories of the various rocks as fracture occurs.

Fragmentation experiments similar to those planned for novaculite will be carried out on Sioux quartzite in the second year and on the other rocks as time and fund permit. The data will be used to check the predictions of the model developed for novaculite. Modifications will be made necessary to allow the model to apply to rocks in general.

SUMMARY

A simple homogeneous rock, Arkansas novaculite, was chosen for dynamic tensile failure studies. Experimental techniques for performing dynamic tensile tests on rocks were developed and used to provide meaningful measurements of dynamic tensile strength. A way to eliminate the occurrence of undesirable radial cracking of the specimen during testing was found; specimen recovery and fracture analysis methods were implemented.

Novaculite specimens were characterized with respect to static and dynamic fracture strength, fracture toughness, defect and microstructure, and other properties and parameters pertinent to the fracture behavior. A particularly important accomplishment was the quantitative determination of the size distribution of inherent cracklike defects, for this is thought to play a dominant role in the comminution characteristics of the rock, and is thus a necessary parameter for a dynamic fracture model. The quasi static tensile strength was determined by means of expanding ring tests to be 440 ± 20 kg/cm^2. The tensile fracture strength of novaculite was measured in high loading rate gas gun experiments to be $_{420}$ ± 20 kg/cm^2 and found to be independent of defect orientation. Thus the tensile fracture strength is strain rate insensitive in the range 10^{-4} to 10^{4} sec^{-1}. A Griffith-Irwin type relation is suggested for the failure criterion under dynamic loads

$$\sigma_f = 10^2 c_{max}^{-1/2}$$

where σ_f is the fracture strength in kilograms/cm^2 and c_{max} is the maximum crack radius in centimeters.

The fracture mechanism in novaculite under dynamic tension was deduced from fractographic observations to consist of the following sequence of events: (1) activation of preexisting cracklike defects, (2) growth of individual cracks radially outward, (3) coalescence of neighboring cracks, and (4) fragmentation of the sample. Based on this

mechanism a dynamic fracture model has been partially developed. According to this model, the most influential parameters affecting the comminution characteristics of rock are the size distribution of preexisting cracks, the applied stress and stress duration, and the inherent fracture resistance of the rock. It is hoped that these quantities can be related by means of the dynamic fracture model to predict resultant fragment size distributions.

During this first year, considerable effort was placed on determination of the quantities associated with the activation and growth stages of the model. In the second year, the crack coalescence and fragmentation stages will be treated, and the dynamic fracture model will be completed. The applicability of the model to rocks in general will be tested by performing experiments on other rock types.

REFERENCES

1. Rinehart, J. S., "Fracture of Rocks," Int. J. Fracture Mech. 2, 534 (1966).
2. Griffith, A. A., "The Phenomena of Rupture and Flow in Solids," Phil. Trans. Roy. Soc. London A221, 163 (1920).
3. Irwin, G. R., "Onset of Fast Crack Propagation in High Strength Steel and Aluminum Alloys," Proceedings 1955 Sagamore Conference on Ordnance Materials, Vol. II (Syracuse University Press, New York, 1956).
4. Irwin, G. R., "Analysis of Stresses and Strains Near the End of a Crack," J. Appl. Mech. 24, 361 (1957).
5. Scheil, E., "Die Berechnung der Anzahl and Grossenverteilung kugelformiger Kristalle in undurchsichtigen Körpern mit Hilfe durch einen ebenen Schnitt erhaltenen Schnittkreise," Z. Anorg. Allgem. Chem. 201 (1931).
6. Scheil, E., " Statistische Gefügeuntersuchungen I," Z. Metallk. 27, 199 (1935).
7. Hopkinson, B., "A Method for Measuring the Pressure Produced in the Detonation of High Explosives or by the Impact of Bullets," Proc. Roy. Soc. A89, 411 (1914).
8. Tetelman, A. S., and A. J. McEvily, Jr., Fracture of Structural Materials, John Wiley, New York, 1967, p. 40.
9. Charest, J. A., D. E. Horne, and B. D. Jenrette, "Phenomenological Considerations of Spall Measurements," APS Bulletin 14, 1170 (1969).
10. Barbee, T. W., L. Seaman, and R. C. Crewdson, "Dynamic Fracture Criteria of Homogeneous Materials," Semiannual Report, Stanford Research Institute, Contract F29601-68-C-0118, November 1969.
11. Butcher, B. M., Spallation of 6061-T6 Aluminum: Behavior of Dense Media Under High Dynamic Pressure, Gordon and Breach, New York, 1968, p. 245.

12. Smith, J. H., "Three Low Pressure Spall Thresholds in Copper," Symposium on Dynamic Behavior of Materials, ASTM, Philadelphia, 1963, p. 264.

13. Warnicka, R. L., "Spallation Thresholds of S-200 Beryllium, ATJ-S Graphite, and Isotropic Boron Nitride at 75°F, 500°F, and 1000°F," MSL-68-18, Materials and Structures Laboratory, General Motors Corporation, Detroit, Michigan, July 1968.

14. Tuler, F. R. and B. M. Butcher, "A Criteria for the Time Dependence of Dynamic Fracture," Int. J. Fracture Mech. 4, 431 (1968).

15. Gilman, J. J., and F. R. Tuler, "Dynamic Fracture by Spallation in Metals," Int. J. Fracture Mech. 6, 169 (1970).

16. Jajosky, B. C. Jr., and M. A. Ferdman, "Spall Studies in Aluminum," AFWL-TR-69-101, Air Force Weapons Laboratory, Kirtland AFB, Albuquerque, New Mexico, September 1969.

18. Skidmore, I. C., "An Introduction to Shock Waves in Solids," Appl. Mater. Res. 4, 131 (1965).

19. Barbee, T., L. Seaman, R. C. Crewdson, "Dynamic Fracture Criteria of Homogeneous Materials," AFWL-TR-70-99, Air Force Weapons Laboratory, Kirtland AFB, Albuquerque, New Mexico, November 1970.

20. Barbee, T., L. Seaman, and D. R. Curran, "Dynamic Fracture Criteria of Homogeneous Materials," AFWL-TR-71-156, Air Force Weapons Laboratory, Kirtland AFB, Albuquerque, New Mexico, December 1971.

21. Curran, D. R., "Dynamic Mechanical Behavior of Iron," in Shock Waves and the Mechanical Properties of Solids, J. J. Burke and V. Weiss, eds., Syracuse University Press, Syracuse, New York 1971.

22. Curran, D. R., and D. A. Shockey, "Dynamic Fracture Criteria for Polycarbonate and Polyimide," DAAD05-71-C-0180, Ballistic Research Laboratory, Aberdeen Proving Ground, Aberdeen, Maryland (Final Report in preparation).

23. Seaman, L., "SRI PUFF 3 Computer Code for Stress Wave Propagation," Technical Report No. AFWL-TR-70-51, Air Force Weapons Laboratory, Kirtland AFB, New Mexico, September 1970.

24. Khvorova, I. V., and A. L. Dmitrik, "An Electron Microscope Study of Siliceous Rocks and Problems of Their Post-Sedimentational Formation," Lithology and Mineral Resources, 1, (1969).

25. Sedlacek, R., "Tensile Fatigue Strength of Brittle Materials," Air Force Materials Laboratory, Wright Patterson AFB, Ohio, Technical Report AFML-TR-66-245, March 1968.

26. Sedlacek, R., and F. A. Halden, "Method of Tensile Testing of Brittle Materials," Rev. Sci. Instr. 33, 298 (1962).

27. Sedlacek, R., "Processing of Ceramics--Surface Finishing Studies," Final Technical Report, Stanford Research Institute, prepared for Naval Air Systems Command, Contract No. N00019-69-C-0229, April 1970.

28. Hardy, R. H., and N. I. Jayaraman, "Hoop-Stress Loading--A New Method of Determining the Tensile Strength of Rock," Am. Inst. of Mining, Metallurgical, and Petroleum Engineers, (1971).

29. Friedman, M., J. Handin, and G. Alani, "Fracture-Surface Energy of Rocks," Texas A&M University Technical Report No. 4, ARPA Contract No. DACA73-68-C-0004, September 15, 1970.

30. Sneddon, I. N., "The Distribution of Stress in the Neighborhood of a Crack in an Elastic Solid," Proc. Roy. Soc. London A187, (1946).

31. Irwin, G. R., "The Crack Extension Force for a Part Through Crack in a Plate," Trans. Amer. Soc. Mech. Engrs., J. Appl. Mech. (1962).

32. Bieniawski, Z. T., "Stability Concept of Brittle Fracture Propagation in Rock," Engin. Geol. 2 (3) 149-162 (1967).

33. Birkimer, D. L., "A Possible Fracture Criterion for the Dynamic Tensile Strength of Rocks," Proceedings 12th Symposium on Rock Mechanics (AIME, New York 1971), p. 573.

34. Keough, D. D., "Development of a High-Sensitivity Piezoresistive Shock Transducer for the Low Kilobar Range," SRI Technical Report, DASA-2508, prepared for Defense Atomic Support Agency, March 1970.

35. Ginsberg, M. J., "Calibration and Characterization of Ytterbium Stress Transducers," SRI Technical Report DASA-2742F prepared for Defense Atomic Support Agency, May 1971.

36. Rinehart, J. S., "Determination of the Dynamic Tensile Strength of Rock," Trans. Amer. Geophys. Union 45, 106 (1964).

37. Mott, N. F., "Fracture of Metals: Some Theoretical Considerations," Engineering, 165, p. 16 (1948).

38. Roberts, D. K., and A. A. Wells, "The Velocity of Brittle Fracture," Engineering 178, 820 (1954).

39. Dulaney, E. N., and W. F. Brace, "Velocity Behavior of a Growing Crack," J. Appl. Phys. 31, 2233 (1960).

40. Berry, J. P., "Some Kinetic Considerations of the Griffith Criterion for Fracture - Parts I and II," J. Mech. Phys. Solids 8, 194-216 (1960).

41. Shockey, D. A., L. Seaman, and J. T. Rosenberg, Monthly Letter Report No. 7 to Air Force Weapons Laboratory, Contract F29601-70-C-0070, Kirtland AFB, Albuquerque, New Mexico, March 15, 1972.

42. Work carried out at the Institut für Festkörpermechanik, 78 Freiburg, 1, Br., Rosastrasse 9, West Germany by H. Schardin, F. Kerkhof, W. Döll, J. F. Kalthoff et al.

APPENDIX

CALCULATION OF THE PEAK AXIAL TENSILE STRESS FROM THE IMPACT VELOCITY (PLEXIGLASS IMPACTING NOVACULITE)

It is assumed that both novaculite and plexiglass are linearly elastic in the stress region of these experiments and that there is no change of slope in the stress-particle velocity curve going from compression to tension. The shock impedances I_s of novaculite and plexiglass are then calculated from the densities ρ_o and sound speeds c_ℓ according to the relation

$$I_s \equiv \frac{\sigma_x}{u_p} = k \rho_o c_\ell \qquad \text{(A-1)}$$

where the densities of novaculite and plexiglass are 2.63 and 1.18 g/cm^3, and the longitudinal sound speeds at peak stress are taken to be 6.00 and 2.80 x 10^3 m/sec, respectively.* The magnitude of k depends on the units used for σ_x and u_p and equals 1.02 x 10^{-2} when stress is measured in kg/cm^2 and velocity in m/sec. The shock impedances so calculated for novaculite and plexiglass are 161 and 33.7 (kg/cm^2)(sec/m), respectively.

The peak axial tensile stress σ_x is given by

$$\sigma_x = I_s^{nov} u_p \qquad \text{(A-2)}$$

or

$$\sigma = \frac{(I_s^{nov})(I_s^{plex})}{I_s^{nov} + I_s^{plex}} U_{proj} \qquad \text{(A-3)}$$

since the particle velocity u_p is related to the impact velocity U_{proj} in the following way

$$I_s^{nov} u_p = - I_s^{plex} (u_p - U_{proj}) \qquad \text{(A-4)}$$

---

* The density and sound velocity of novaculite were measured in this work as described in Section III. The data for plexiglass are the results of Barker and Hollenbach, J. Appl. Phys. 41, 4208 (1970).

Substituting the above calculated values of shock impedance into Eq. (A-3) we obtain the following expression,

$$\sigma_x = 27.9\ U_{proj} \quad , \qquad \text{(A-5)}$$

which is used to calculate the peak axial compressive stress in novaculite in kg/cm^2 from the impact velocity in m/sec. For the experiments with a free surface, the peak compressive stress should be equal in magnitude to the peak tensile stress, assuming the tensile strength is not exceeded. If a low impedance backing material is used, the peak tensile stress in the specimen will be equal in magnitude to the difference between the peak compressive stress in the specimen and that reached in the backing material.

The stress values calculated, using Eq. (A-5), from the measured impact velocities in this work are tabulated in Tables II and III and are considered accurate to about 4%, excluding effects of impact tilt and material non-uniformities.